NREL/TP-451-7189 • UC Category: 1263 • DE95000244

Polycrystalline $CuInSe_2$ and CdTe PV Solar Cells

Annual Subcontract Report
15 April 1993 – 14 April 1994

N. G. Dhere
Florida Solar Energy Center
Cape Canaveral, Florida

NREL technical monitor: B. von Roedern

National Renewable Energy Laboratory
1617 Cole Boulevard
Golden, Colorado 80401-3393
A national laboratory of the U.S. Department of Energy
Managed by Midwest Research Institute
for the U.S. Department of Energy
under contract No. DE-AC36-83CH10093

Prepared under Subcontract No. XG-2-11036-5

November 1994

NOTICE

Available to DOE and DOE contractors from:
Office of Scientific and Technical Information (OSTI)
P.O. Box 62
Oak Ridge, TN 37831
Prices available by calling (615) 576-8401

Available to the public from:
National Technical Information Service (NTIS)
U.S. Department of Commerce
5285 Port Royal Road
Springfield, VA 22161
(703) 487-4650

TABLE OF CONTENTS

LIST OF FIGURES

SUMMARY

Objectives

The principal objective of the research project is to develop novel and low-cost processes for the fabrication of stable and efficient $CuIn_{1-x}Ga_xSe_2$ and CdTe polycrystalline-thin-film solar cells using reliable techniques amenable to scale-up for economic, large-scale manufacture. The aims are to develop a process for the non-toxic selenization so as to avoid the use of extremely toxic H_2Se in the fabrication of $CuIn_{1-x}Ga_xSe_2$ thin-film solar cells; to optimize selenization parameters; to develop a process for the fabrication of CdTe solar cells using Cd and Te layers sputtered from elemental targets; to develop an integrated process for promoting the interdiffusion between Cd/Te layers, CdTe phase formation, grain growth, type conversion, and junction formation; to improve adhesion; to minimize residual stresses; to improve the metallic back-contact; to improve the uniformity, stoichiometry, and morphology of $CuIn_{1-x}Ga_xSe_2$ and CdTe thin films; and to improve the efficiency of $CuIn_{1-x}Ga_xSe_2$ and CdTe solar cells.

Discussion

This is an annual technical report on the Phase II of a three-year phased research program. FSEC has established a well-equipped laboratory with hazardous material handling capabilities for research and development on thin-film solar cells. PV modules based on $CuIn_{1-x}Ga_xSe_2$ and CdTe polycrystalline thin films have been targeted as likely candidates for low-cost energy production by the U.S. Department of Energy and a segment of PV industry. They offer low material cost, potential scalability and automation of the fabrication processes, and efficiencies competitive with the presently predominant crystalline-Si technology. High efficiency $CuIn_{1-x}Ga_xSe_2$ and CdTe solar cells are based on coevaporated or sequentially evaporated Cu, In, Ga metallic precursors and close-space sublimated CdTe thin films. Both these processes are difficult to scale-up for large-scale, economic manufacture. Sputtering of Cu-In-Ga metallic precursors as well as elemental Cd and Te layers, on the other hand can be easily scaled up and hence is the preferred industrial process for thin-film deposition. $CuIn_{1-x}Ga_xSe_2$ is a pseudo-quaternary analog of the ternary compound $CuInSe_2$ in which gallium is substituted on some indium sites which serves to raise the bandgap towards the theoretical optimum value of 1.5 eV. Gallium-indium form a low temperature eutectic with the eutectic point at ~17° C. Indium-gallium or gallium layers would invariably result in liquid or liquid-like behavior destroying the structural stability. A new process being developed at FSEC can solve the problem of incorporation of gallium without encountering the deleterious interaction between indium and gallium. In this process, the difficulty of low-melting point precursors has been avoided by incorporating gallium using a single Cu-Ga(22 at.%) alloy target. Internal stresses in refractory metal Mo films prepared by magnetron sputter deposition depend strongly on the working gas pressure. A higher working gas pressure is expected to moderate the flux and energy of these particles.

Cd, Te, high temperature (~450° C, for >15 minutes), oxygen, and $CdCl_2$ are essential ingredients for the fabrication of CdTe solar cells. A blocking contact and especially the formation of a

junction away from the CdTe\CdS interface often have been found to result in low efficiencies. Even though standard recipes have been developed for obtaining high efficiency solar cells from several of the other processes, the processing details need to be developed for each new process so as to achieve high conversion efficiencies.

Magnetron-sputter-depositions of Mo and Cu-In-Ga metallic precursor films were carried out in a 18" diameter and 24" height bell jar. Cd and Te layers were magnetron-sputtered in a 6-way 6" diameter cross type chamber pumped with a turbomolecular pump. Soda-lime float glass was used as the substrate for the fabrication of the solar cells. The Cu/In films were subjected to a *in situ* heat treatment at 80-90° C for 10 min. A novel two-selenization process using Se vapor has been developed for achieving recrystallization of Cu-rich precursor during the first selenization and conversion of $Cu_{2-x}Se$ phase at the surfaces and grain boundaries during the second selenization of Cu-poor precursor. Initially the composition aimed at was $Cu_{0.85}In_{1-x}Ga_xSe_2$. In this process initially 80% of Cu-Ga was deposited on molybdenum followed by 25% of In and then 10% of Cu-Ga intended to avoid the globule formation of In and In-Ga. A higher selenization temperature of 550° C was found to be essential for improving the properties of the thin films and solar cells. The two-selenization process improved the adhesion to Mo back-contact layer considerably. Experiments carried out to increase the bandgap by adding gallium to form selenized $CuIn_{1-x}Ga_xSe_2$ thin films with $x \approx 0.2$-0.25 also improved film adhesion still further. The combination of two-selenization process and Ga addition near Mo contact have virtually eliminated the vexing problem of peeling off. Using the two selenization process, well-adherent $CuIn_{1-x}Ga_xSe_2$ thin films free from pin-holes are being prepared routinely.

Estimates of composition were made by measuring the resistance of selenized $CuInSe_2$ and $CuIn_{1-x}Ga_xSe_2$ thin films. Initially 90% of copper-gallium was deposited, followed by 25% indium and then selenized at a temperature of 500-550° C. A series of experiments were carried out to obtain the desired composition and a compact, large-grain microstructure. A discontinuous copper- gallium layer at the top was avoided by increasing the thickness of Cu-Ga top layer. From the electron probe microanalysis the composition was found to be closer to the desired composition of Cu:In:Ga:Se of 22.95:25.03:1.40:50.63. The measured resistance was about 50-80 KΩ. Morphology of precursors and $CuIn_{1-x}Ga_xSe_2$ thin films was studied because of their effect on photovoltaic properties of solar cells. Very small sub-grain features were studied for the *first time* by atomic force microscopy, and quantitative data on rms roughness and 3-d images were obtained. Morphology of precursors was found to change from initial very smooth layers with 200-300 Å size features and a rms surface roughness of <10 Å, to 3-d ~9000 Å size islands, coalescing grains with a fine sub-grain structure, and finally to compact, well-faceted, large-grain $CuIn_{1-x}Ga_xSe_2$ thin films with rms roughness in the range 950-1500 Å.

Several cells were completed and measured at IEC by deposition of thick CdZnS:In\ITO\Ni fingers on glass\Mo\$CuIn_{1-x}Ga_xSe_2$ samples prepared at FSEC. The best cell obtained with films prepared using precursors homogenized *in situ* prior to selenization gave an open circuit voltage V_{oc} of 377 Mv, J_{sc} of 34.8 Ma, a fill factor 62.5% and active area conversion efficiency of 8.2%. Spectral response was found to be fairly constant over the entire spectral range. A few cells were also completed at NREL by deposition of thin CBD CdS\ZnO:Al\Ni-Al grid contact on

glass\Mo\$CuIn_{1-x}Ga_xSe_2$ samples prepared at FSEC. The V_{oc} of the cells was in the 370-388 mV range. The best cell showed J_{sc} of 31.5 mA, fill factor of 45.1% and the total area efficiency of 5.87%.

Most of the groups are using commercial SnO_2:F coated sodalime glass substrates for CdTe solar cells. Chemical bath deposition (CBD) technique has been well-developed at FSEC and CdS layers for CdTe solar cells are being prepared routinely from acetate reactants. Considerable work was carried out on the magnetron-sputter deposition of Cd and Te layers, suitability of targets for sputtering of tellurium, heat treatments in various ambients such as vacuum and partial pressures of nitrogen, nitrogen-oxygen, and helium-oxygen mixtures for phase formation and grain growth. Vacuum melted targets and adequate thermal and electrical contact between the magnetron sputtering source and Te target and efficient water cooling were found to be essential for well-controlled Te deposition at high deposition rates. It is estimated that using this technique, higher and controllable deposition rates could be employed to allow deposition of elemental Cd\Te layers required to form >4 μm thick CdTe film in <4 min. Elemental stacks consisted of first and last Te layers so as to obtain better adhesion and to minimize Cd reevaporation. Experiments were conducted with stoichiometric Cd/Te layers and excesses ranging from 10% Cd-rich to 30% Te-rich. Most experiments were carried out with small excesses of Te to promote p-type conductivity. XPS analysis showed the presence of traces of CdTe even in as-deposited Cd\Te layers on unheated substrates. Complete CdTe phase formation was observed by XRD and XPS analysis after heat treatment at temperatures <300° C for 30 minutes of Cd/Te elemental layers with a small excess Cd or Te. CdS\CdTe interface and junction formation was promoted by heat treatments at 450-475° C. Excessive problems of peeling-off and pinhole formation encountered for heat treatments at temperatures >440° C were resolved by using thicker CdS layers. A semi-closed graphite crucible and 5-30% Te excess with a Te top layer were used to minimize Cd and even Te reevaporation at temperatures over 440° C. Peeling off problems were frequent in heat treatment of Cd/Te elemental stack deposited on $CdCl_2$-coated glass\$SnO_2$:F\CdS samples especially because of the hygroscopic nature of $CdCl_2$. Peeling off problems were considerably reduced when $CdCl_2$ was applied on to Cd/Te stacks on glass\$SnO_2$:F\CdS samples. Tellurium oxide and cadmium chloride were detected by XPS analysis at considerable depths in the $CdCl_2$-treated Te-rich samples and heated in oxygen-containing ambients at 350-450° C. Based on empirical observations, the heat treatment ambients were optimized. Finally this has made it possible to routinely prepare well-adherent and mostly pinhole-free CdTe layers on glass\$SnO_2$:F\CdS samples. These films are considerably robust as compared to CdTe films deposited by other low-temperature processes. CdTe cells were completed after $CdCl_2$ treatment by applying doped graphite paste, and silver paste contacts. Some of the cell completion was carried out at NREL. CdTe thin-films Solar cells prepared after low-temperature (≤400° C) heat-treatments showed V_{oc} of 320-380 mV, J_{sc} of ~5 mA and a poor FF values of ~30%. Solar cells prepared using high-temperature-treated CdTe layers showed V_{oc} of >580 mV, however with low J_{sc} and poor fill factor values most probably resulting from blocking contacts or junction formation away from the CdTe\CdS interface.

INTRODUCTION

This is an annual technical report on the Phase II of a three-year phased research program. $CuIn_{1-x}Ga_xSe_2$ and CdTe polycrystalline-thin-film solar cells are emerging as the leading candidates for meeting the DOE long-range cost goals. FSEC has established a well-equipped laboratory with hazardous material handling capabilities for research and development on thin-film solar cells. The principal objective of the research project is to develop novel and low-cost processes for the fabrication of stable and efficient $CuIn_{1-x}Ga_xSe_2$ and CdTe polycrystalline-thin-film solar cells using reliable techniques amenable to scale-up for economic, large-scale manufacture. The aims are to develop a process for the non-toxic selenization so as to avoid the use of extremely toxic H_2Se in the fabrication of $CuIn_{1-x}Ga_xSe_2$ thin-film solar cells; to optimize selenization parameters; to develop a process for the fabrication of CdTe solar cells using Cd and Te layers sputtered from elemental targets; to develop an integrated process for promoting the interdiffusion between Cd/Te layers, CdTe phase formation, grain growth, type conversion, and junction formation; to improve adhesion; to minimize residual stresses; to improve the metallic back-contact; to improve the uniformity, stoichiometry, and morphology of $CuIn_{1-x}Ga_xSe_2$ and CdTe thin films; and to improve the efficiency of $CuIn_{1-x}Ga_xSe_2$ and CdTe solar cells.

1.1 Background

Photovoltaic (PV) modules based on polycrystalline thin films have been targeted as likely candidates for low-cost energy production by the U.S. Department of Energy (DOE) and a segment of PV industry. Several polycrystalline thin-film materials such as Cu_2S, CuO, CdTe, $CuIn_{1-x}Ga_xSe_2$, and Zn_3P_2 have been investigated for PV applications. However, only $CuIn_{1-x}Ga_xSe_2$ and CdTe have emerged as strong potential candidates for low-cost, large-scale manufacture of PV solar cells. They offer low material cost, potential scalability and automation of the fabrication processes, and efficiencies competitive with the presently predominant crystalline-Si technology.

Of the several processes employed for the preparation of $CuIn_{1-x}Ga_xSe_2$ thin films, vacuum coevaporation, selenization of sputtered metallic precursors, and rapid isothermal processing have resulted in device efficiencies over 10%, the present best efficiency being 16.4% [1-4]. CdTe has long been recognized as an important PV material for the fabrication of low-cost, high efficiency solar cells because of its near-ideal bandgap of 1.5 eV and high optical absorption coefficient [5-7]. PV conversion efficiencies over 10% have been achieved by most of the over fifteen processes employed for the deposition of CdTe thin films, the best efficiency being 15.8% by close-space sublimation (CSS) on borosilicate glass substrates coated with high quality SnO_2:F window layers [1,5-11]. $CuIn_{1-x}Ga_xSe_2$ thin-film solar cells which are fabricated in the substrate configuration usually consist of ~1 μm Mo layer on low-cost sodalime glass by sputtering or e-beam evaporation, followed by $CuIn_{1-x}Ga_xSe_2$ absorber (usually with $x = 0.25$, at times with sulfur with a formula $CuIn_{1-x}Ga_xSe_{2-y}S_y$), a thin heterojunction partner CdS layer by solution growth, transparent conducting ZnO:Al window by sputtering or metalorganic chemical vapor deposition (MOCVD), and Ni\Al front grid vacuum evaporated through a mechanical mask. CdTe solar

cells fabricated in the superstrate structure usually consist of 7059 borosilicate or sodalime glass coated with SnO_2:F transparent conducting window, heterojunction partner CdS layer grown by chemical bath deposition (CBD), CdTe absorber layer, and back contact of doped graphite and silver paste.

Siemens Solar Inc (SSI), International Solar energy Technology (ISET), and Energy Photovoltaics (EPV) all in USA have been fabricating large-area thin-film $CuIn_{1-x}Ga_xSe_2$ modules with the best power outputs of 43.1 W from 3832 cm^2 (SSI) and 10.4 W from 938 cm^2 (SSI), 4.8 W from 846 cm^2 (ISET), and 5.7 W from 791 cm^2 (EPV) [1,12-14]. The key strength of emerging $CuIn_{1-x}Ga_xSe_2$ thin-film technology is their stability verified at NREL for over 4 years. Golden Photon Industries (GPI) and Solar Cells Inc (SCI) in the US, Matsushita Battery in Japan, and BP Solar in UK are actively developing CdTe module fabrication with sizes ranging from 1-8 ft^2. Absorbers are deposited by spray (GPI), elemental vapor deposition (SCI), screen printing (Matsushita), and electrodeposition (BP Solar) [10,15-17]. The reported large-area module power outputs are 27.5 W from 3528 cm^2 (GPI), 53.1 W from 6879 cm^2 (SCI), 10.0 W from 1200 cm^2 (Matsushita), and 38.2 W from 4540 cm^2 (BP Solar). Both GPI and SCI have announced plans to construct large multimegawatt plants. Health, safety, and environmental aspects, recycling of cadmium and selenium from PV modules and manufacturing waste, and disposal in municipal landfill sites in EC and USA are being constantly studied [18,19]. Both the qualifications of "promised low cost technology" and "high efficiency" must be met simultaneously for the realization of the potential of $CuIn_{1-x}Ga_xSe_2$ and CdTe PV modules. With the recent demonstration of record efficiencies of 16.4% for $CuIn_{1-x}Ga_xSe_2$ and 15.8% for CdTe, development of novel, low-cost processing techniques, scalable for economic large-area production at a reasonable throughput assumes vital importance.

High efficiency $CuIn_{1-x}Ga_xSe_2$ and CdTe solar cells are based on coevaporated or sequentially evaporated Cu, In, Ga metallic precursors and close-space sublimated CdTe thin films. Both these processes are difficult to scale-up for large-scale, economic manufacture. Sputtering of Cu-In-Ga metallic precursors as well as elemental Cd and Te layers, on the other hand can be easily scaled up and hence is the preferred industrial process for thin-film deposition. Sputtering is a vacuum-coating process in which material is dislodged and ejected from the surface of a solid or a liquid due to the momentum exchange associated with surface bombardment by energetic particles. A source of coating material called the target is placed in a vacuum chamber along with the substrates, and the chamber is evacuated to a pressure typically in the range of 5×10^{-4} to 5×10^{-7} Torr. The bombarding species are generally ions of a heavy inert gas like argon. The sputtered material is ejected primarily in atomic form. The substrates are positioned in front of the target so that they intercept the flux of sputtered atoms. The most striking characteristic of the sputtering process is its universality. Since the coating material is passed into the vapor phase by a mechanical (momentum exchange) rather than a chemical or thermal process, virtually any material is a candidate for coating. DC methods are generally used for sputtering metals. An rf potential must be applied to the target when sputtering non conducting materials. Depending on the application, the sputtering apparatus can assume an almost unlimited variety of configurations. The inherent advantages of magnetron sputtering over other conventional thin film deposition techniques include i) large area coverage, ii) very high deposition rates, iii) low

substrate temperature, and iv) ease of process control.

The formation of thin films involves the process of nucleation and growth. There are following three basic growth modes: i) Island or Volmer-Weber, ii) Layer or Frank-van der Merve, iii) Layer followed by three-dimensional islands or Stranski-Krastanov. Island growth occurs when the smallest stable clusters nucleate on the substrate and grow in three dimensions to form islands. This happens when atoms or molecules in the deposit are more strongly bound to each other than to the substrate. The opposite characteristics are displayed during layer growth. Here the extension of the smallest stable nucleus occurs overwhelmingly in two dimensions resulting in the formation of planar sheets. In this growth mode the atoms are more strongly bound to the substrate than to each other. The layer plus island or Stranski-Krastanov growth mechanism is an intermediate combination of the aforementioned modes. In this case, after forming one or more monolayers, subsequent layer growth becomes unfavorable and islands form. In most cases of deposition on dissimilar substrates, island (Volmer-Weber) or initial layer plus island (Stranski-Krastanov) growth is usually observed. In these cases, after exposure of the substrate to the incident vapor, a uniform distribution of small but highly mobile clusters or islands are observed. In this stage the prior nuclei incorporate impinging atoms and subcritical clusters and grow in size while the island density rapidly saturates. The next stage involves merging of the island by a coalescence phenomenon that is liquid-like in character especially at high substrate temperatures. Coalescence decreases the island density, resulting in local denuding of the substrate where further nucleation can occur. Crystallographic facets and orientation are frequently preserved on islands and at interfaces between initially disoriented, coalesced particles. Coalescence continues until a connected network with unfilled channels in between develops. In some cases, a secondary nucleation can take place on an existing island leading to a fine subgrain structure. With further deposition, the channels fill in and shrink, leaving isolated voids behind. Finally, even the voids fill in completely, and the film is said to be continuous. Indium with a melting point of ~157° C, is known to have a strong tendency to form 3-dimensional islands or globules.

1.2 Copper-Indium-Gallium-Diselenide thin-film Solar Cells

As mentioned above $CuInSe_2$ is one of the most promising absorber materials for thin film solar cells. However, it has an optical bandgap of 1.04 eV which is smaller than the theoretical optimum value of 1.5 eV. $CuIn_{1-x}Ga_xSe_2$ is a pseudo-quaternary analog of the ternary compound $CuInSe_2$ in which gallium is substituted on some indium sites which serves to raise the bandgap to values between 1.04-1.7 eV. Increasing the bandgap by alloying with gallium gives room for further optimization with respect to adapting the bandgap to the solar spectrum. However, with higher gallium content ($x > 0.3$ in $CuIn_{1-x}Ga_xSe_2$) the photovoltaic performance of heterojunctions with this absorber material deteriorates not only because it is difficult to find an appropriate window but also because the minority carrier transport in the film falls off [20]. Since gallium has a melting point of 30° C it needs to be sputtered as a liquid, making the process inefficient. Gallium-indium form a low temperature eutectic with the eutectic point at ~17° C. Indium-gallium or gallium layers would invariably result in liquid or liquid-like behavior destroying the structural stability.

Internal stresses in refractory metal Mo films prepared by magnetron sputter deposition depend strongly on the working gas pressure. A general feature is a transition pressure below which the films are in compression, whereas above this pressure the films have tensile stress [21]. It has been suggested that such stress reversals are dependent on energetic bombardment by reflected neutrals and sputtered atoms. A higher working gas pressure is expected to moderate the flux and energy of these particles. At relatively low pressures the arriving atoms have higher kinetic energy and the resulting film has dense microstructure, experiencing compressive stress.

The methods of physical vapor deposition of coevaporated or sequentially evaporated metallic species in the presence of Se vapor flux have been highly successful in achieving high efficiencies [3,4]. However, the industrial participants have opted for the more scalable selenization of metallic precursors by H_2Se or Se vapor for large-area PV module fabrication. Selenization of Cu-In metal films has already been proven to be a suitable production process for polycrystalline $CuInSe_2$ thin films in photovoltaic application. One of the successful method of selenization was by using H_2Se as a reactant. However, this approach faces high environmental and technological costs in overcoming high toxicity of H_2Se ambient. Szot and Prinz [22] have found an alternative technique to produce large area $CuInSe_2$ thin films based on elemental selenium chalcogenization with a Se film deposited as a reactant. The process of selenization using selenium layer or vapor is not very well understood.

The poor adhesion to molybdenum coated substrates has been attributed to a three fold volume expansion during selenization. The problem is especially acute in the case of electrodeposited films in which Cu/In layers consist mostly of two separate elemental phases. In evaporated and also in sputtered films, the significant alloying between Cu-In layers during the deposition seems to result in an approximately two fold volume expansion even on uncooled substrates. The additional expansion during selenization of these films may not produce excessive stress and hence the problem of peeling off could be minimized. Large grain $CuInSe_2$ thin films prepared by coevaporation maintaining initially a higher proportion of copper followed by a higher proportion of indium in the second phase have resulted in a higher efficiency.

1.3 Cadmium-Telluride Thin-Film Solar Cells

Low dopant density is an important issue in CdTe solar cells. CdTe layers prepared by most techniques are mostly intrinsic or lightly ($4\text{-}8\times10^{14}$ cm^{-3}) p-type doped compared to typical p-type doping of $CuIn_{1-x}Ga_xSe_2$ of $>10^{16}$ cm^{-3} [23]. Wide bandgap semiconductors such as CdTe and ZnTe have a tendency to self-compensate shallow levels of deliberately incorporated extrinsic donor or acceptor impurities through spontaneous generation of native point defects, such as vacancies, antisite defects, host interstitials, or their complexes. Deliberate extrinsic doping moves the Fermi level E_F close to the conduction or the valence band and creates a metastable phase. The metastable phase could be brought to the equilibrium state by minimizing the total free energy of the system by generating a collection of native defects with appropriate ionization levels in the bandgap and letting the free carriers from the Fermi sea into these levels bringing back the Fermi level to the intrinsic level E_i [24,25]. Self-compensation has been avoided by

several methods such as plasma-assisted doping of ZnSe with nitrogen and by introducing dopants at concentrations far above the equilibrium thermodynamic limits [26]. However, self-compensation may occur by creation of native defects during subsequent heat treatment carried out to anneal the defects. Type conversion of as-deposited n-type CdTe to p-type and junction formation between CdS\CdTe are achieved by annealing in oxygen containing ambient at 400-500° C [17,27,28]. Without the oxygen, the cells behave like buried-homojunction CdTe cells and have substantially lower performance. Fast cooling rates are employed after oxygen and $CdCl_2$ heat-treatment to freeze the dopants without the problem of self-compensation [29].

A key step in fabricating high efficiency CdTe cells using a low-temperature process such as sputtering, vacuum evaporation, and laser ablation is the post-deposition $CdCl_2$ treatment consisting of application of $CdCl_2$:methanol solution by immersion or by placing drops on the film followed by heating at 400° C in air for 30 min. It increases CdTe grain size and promotes the formation of mixed CdS\CdTe interface region by interdiffusion [30]. A broadened interface layer has been observed for heat treatments in the presence of oxygen and especially with $CdCl_2$ treatment [31]. Distinct mixed interface layers viz. $CdS_{1-x}Te_x$ and CdS_yTe_{1-y} have been observed during the processing of cells [32]. A good junction formation is essential for achieving high efficiencies. High efficiency and excellent diode factor were observed in CdS\CdTe cells grown by atomic layer epitaxy (ALE), even though a mixed ALE $CdS_{1-x}Te_x$ layer limited the low wavelength response [8,23]. Thus Cd, Te, high temperature (~450° C, for >15 minutes), oxygen, and $CdCl_2$ are essential ingredients for the fabrication of CdTe solar cells [11,17,28,33]. A blocking contact and especially the formation of a junction away from the CdTe\CdS interface often have been found to result in low efficiencies [28,31]. Even though standard recipes have been developed for obtaining high efficiency solar cells from several of the other processes, the processing details need to be developed for each new process so as to achieve high conversion efficiencies.

2. TECHNICAL DISCUSSION

Magnetron-sputter-depositions of Mo and Cu-In-Ga metallic precursor films were carried out in a 18" diameter and 24" height bell jar. A cryopump having a very high argon-pumping capacity was employed for sputtering. Cd and Te layers were magnetron-sputtered in a 6-way 6" cross type chamber pumped with a turbomolecular pump. Initially a vacuum in the range of $8\text{-}10\times10^{-3}$ Torr was obtained using two-stage rotary pumps lubricated with a corrosion-resistant fluorocarbon pump fluid. The chambers were then pumped with the cryopump or turbo-molecular pumps. The chosen cryopump and turbomolecular pump have very high pumping speeds for water, other vapors, nitrogen, oxygen, thus providing clean vacuum reasonably free of water and hydrocarbon vapors.

The 18" diameter chamber has three, 3 inch diameter water-cooled planar magnetron sputtering sources and the 6" 6-way cross chamber has two, 3 inch diameter water-cooled planar magnetron sputtering sources. The systems are equipped with a dc power supply (1 KW) and a rf power supply (750 W) with an air cooled matching network. Process control and data acquisition is carried with a microcomputer, data acquisition cards, and RS232 interfaces. Capacitance and

convectron gauges with a vacuum gauge control unit are utilized to monitor the pressures in the chambers and the backing lines. The flow rate of sputtering gas (Ar 99.998%) was controlled by mass flow controllers (0-200 sccm).

2.1 $CuIn_{1-x}Ga_xSe_2$ Thin-Film Solar Cells

The structure of $CuInSe_2$ thin film solar cells consisted of glass/Mo/$CuInSe_2$/CdS/ZnO:Al/Al contact fingers. The process chart shown in Figure 1 gives an overall view of the entire process that leads to the fabrication of a $CuIn_{1-x}Ga_xSe_2$ thin film solar cell. Each process has been explained below:

Soda-lime float glass kindly supplied by Libbey Owens Ford (LOF) was used as the substrate for the fabrication of the solar cells. Soda-lime float glass pieces of sizes 1½" x 1½" or 1" x 1" were cut from large sheets for use in the deposition of various layers. The glass substrates were initially cleaned with a window cleaner followed by liquinox neutral soap solution. Mechanical brushing with the liquinox solution enhanced the adhesion of the film to the substrate. The substrates were then cleaned in distilled and deionized water. They were then placed overnight in a bath containing KOH:ethanol solution. The substrates were then rinsed in deionized water followed by ultrasonic cleaning in isopropyl alcohol for about 5 minutes. Following this the substrates were placed in boiling deionized water. At the end of the cleaning process the substrates were dried and weighed.

2.1.1 Deposition of Molybdenum Thin Films

Molybdenum used as back contacts were deposited by dc magnetron sputtering. Molybdenum depositions were carried out in the 18" diameter chamber. Experiments were carried out by varying the different process parameters. In one experiment, multiple power variation was carried out. In this case a 1.3 μm film was obtained by alternately sputtering at 50 W for 2 minutes followed by sputtering at 100 W for 5 minutes. But when the depositions were carried out at 50 W for 1 minute and at 100 W for 2.5 minutes the films were found to peel off at greater thicknesses. The argon pressure in both the experiments was adjusted at 1 x 10^{-2} Torr in the convectron gauge while the capacitance gauge which is an absolute pressure manometer showed a reading of 1.6 x 10^{-2} Torr. In the third set of experiments, a new substrate holder was fabricated to carry out three depositions in one run. Molybdenum was deposited at higher sputtering pressure in the range of 1.5 x 10^{-2} Torr and lower sputtering power of 50 W. In this case the molybdenum atoms were made incident at angles of -45°, 0°, +45°. Some molybdenum coated samples were kindly supplied by Siemens Solar Inc.

The films deposited at a pressure of 5 x 10^{-3} Torr and high sputtering power possessed considerable compressive stress. Hence there were problems of peeling off in molybdenum layers due to the residual stress. Some molybdenum films showed cracking and peeled off partially as the thickness was increased to the desired range of 0.9-1.5 μm. Initially molybdenum thin films were deposited at higher power and lower pressure. To minimize the stress further depositions were carried at increasing pressures and lower power values. It was found that it was

possible to obtain a 1.5 μm thick molybdenum film using the lower power and higher pressure.

2.1.2 Deposition of Copper, Indium, and Gallium

Copper, Indium, and copper-gallium thin films were deposited on 1½" x 1½" or 1" x 1" Mo-coated soda-lime float glass substrates. These depositions were also carried out in the 18" diameter chamber. Initially it was expected that there would be problems due to the surface melting and splattering of the indium target at high sputtering power. But due to the efficient cooling of the sputter guns no such problem was encountered. The optimization process involved calibrating the deposition rate with sputtering power.

The Cu/In films they were subjected to a *in situ* heat treatment in high vacuum immediately after the deposition. This process was carried out to promote a proper intermixing of Cu/In precursor layers before selenization. Experiments were carried out to study the various phase changes in Cu/In layers by *in situ* heat-treatments. Time temperature profiles were varied with the maximum temperature in the range of 80-155° C. Temperature in excess of the melting point of indium (~156° C) was found to be detrimental to the formation of a uniform precursor layer.

In cases of substrates subjected to temperatures of about 10-20° C below the melting point of indium, a reaction zone was found to pass through the film. There were cases of globule formation at certain higher temperatures. This was found to be detrimental to the completed solar cell. The microglobule formation and pitting was attributed to a small fraction of highly activated, mobile atoms at temperatures above 0.8 T_m (T_m is the melting point of indium) moving over the surface 10 to 100 times the interatomic distance before losing their kinetic energy. Intermixing of Cu/In precursor layers were studied by Rutherford backscattering (RBS) and X-ray photoelectron spectroscopy (XPS). For the RBS analysis, Cu/In thin films were deposited on single crystalline silicon wafers having a 1 μm thick thermally grown SiO_2 surface layer. The RBS spectra clearly indicated that preheating leads to a homogeneous intermixing but it also shows that there is some diffusion taking place even at room temperature. The XPS spectra showed the region near molybdenum to be copper rich.

During the later stage, a two-selenization process was developed in which the initial deposition was carried out to make the film copper rich. A copper rich layer increases the grain size but it should be avoided near the junction because it will lead to copper whisker formation. At the same time an indium rich layer will lead to a uniform grain structure. Initially $Cu_{0.85}In_{0.25}$ was deposited followed by the preheating. Rutherford back-scattering (RBS) analysis was carried out to obtain estimates of the individual layer thicknesses and the extent of intermixing of the precursor layers. $Cu_{0.85}In_{0.25}$ depositions were carried out on Si/SiO_2 samples of size 1"x 1½". Two samples were prepared in which one of them was subjected to preheating while the other was not. Composition information was also obtained from XPS.

2.1.3 Selenization Process

Selenization was carried out by evaporating selenium over Cu/In bilayers in a vacuum chamber.

Selenium was evaporated from a Knudsen cell type molybdenum boat (2½" x ½" x 1 ½") on to a sample mounted under a ceramic plate heater. An old vacuum system donated by Martin Marietta Missile Systems was refurbished and made available for selenization. High vacuum in the range of $< 10^{-6}$ Torr was obtained routinely in this vacuum system pumped with a diffusion pump. The system was fitted with electrodes and holders for vacuum evaporation using a power supply. There was also a liquid nitrogen trap which prevented backstreaming of diffusion-pump oil vapor to the substrates and at the same time minimized the amount of selenium vapor reaching and damaging the pumps. A better control of the selenization process was possible because of the high vacuum, larger size and better accessibility. A ceramic heater was placed on top of the samples. Since the heating was done in vacuum, the heat transfer was by radiation. To prevent any heat losses the heater was enclosed in a stainless steel shield. The substrate itself was placed on a substrate holder supported by a stainless steel cylinder which was used to contain the spread of selenium vapor to other regions of the chamber.

According to the cosine law of emission the mass deposited per unit area is given by [34]

$$\frac{dM_r(\varphi,\theta)}{dA_r} = \frac{M_e}{\pi r^2}\cos\varphi\cos\theta \qquad (2.1)$$

$$\frac{d(thickness)}{dA_r} = \frac{M_e}{\rho\pi r^2} \qquad (2.2)$$

where r is the distance between the substrate surface and the boat, ρ is the density of selenium, θ is the angle of incidence and φ angle of the normal to the surface element dA_e. Initially the distance r was adjusted to be ~2½". During the initial experiments, the heat radiated from the substrate and substrate holder, being heated to high temperatures, increased the selenium evaporation rate excessively. There were frequent problems of peeling off in the case of high deposition rates (> 300 Å/sec). The distance was, therefore increased to ~3½" so as to obtain an independent control of selenium evaporation rate. In the initial experiments, a backing plate was placed over the substrate and below the heater for uniform heat distribution. However, in some cases, the stress caused by the weight of the backing plate caused breakage of glass, at the high processing temperatures. Hence the backing plate was removed.

In the selenization process the selenium boat is slowly heated to the desired current to obtain a selenium evaporation rate in the range of 25-50 Å s^{-1}. Once the required selenium evaporation rate is obtained, the temperature is ramped to 450-550° C at a rate of 50° C min^{-1}. This temperature is maintained for about 20-30 minutes. Then it is slowly cooled at the rate of 10° C min^{-1} to about 350-360° C with continued selenium evaporation. Then finally it is cooled to the room temperature without selenium evaporation. Problems were encountered in controlling the boat current because of the molten selenium charge carrying large currents during parts of the evaporation. The power to sample-heater was calibrated so as to reach the temperature of 450-550° C during the selenization process. Proper control of the selenization temperature and

time was necessary to avoid indium selenide loss from and selenium deficiency from under selenization.

Compact, large-grain morphology achieved by recrystallization of the Cu-rich precursors with the help of a binary copper chalcogenide Cu_xSe ($x < 2$) which has a melting point of 523° C and which acts as a flux with high diffusion coefficient for species involved in the growth process is an important ingredient of the recent high efficiency processing [35]. Secondly, higher efficiencies have been achieved by increasing the bandgap with Ga incorporation. The various processing paths being pursued for the preparation of high efficiency $CuIn_{1-x}Ga_xSe_2$ are suitable only when the metallic species are coevaporated or sequentially evaporated in the presence of a Se flux because of solid phase formation with an accompanying Se flux on heated substrates. None of these paths can be followed in the post-selenization of metallic precursors deposited on unheated substrates especially they involve deposition of Ga or Ga + In [1,3,4,35]. As discussed above, incorporation of gallium in the metallic precursor deposited on unheated substrates poses a serious problem because of the low (~30° C) melting point of gallium and the formation of low (~17° C) melting point In-Ga eutectic. A new process being developed at FSEC can solve the problem of incorporation of gallium without encountering the deleterious interaction between indium and gallium. In this process, the difficulty of low-melting point precursors has been avoided by incorporating gallium using a single Cu-Ga(22 at.%) alloy target.

A novel two-selenization process has been developed for achieving recrystallization of Cu-rich precursor during the first selenization and conversion of Cu_xSe phase at the surfaces and grain boundaries during the second selenization of Cu-poor precursor. Experiments were carried out to improve the grain size of $CuInSe_2$ by first selenizing a Cu(rich)-In layer having Cu proportions of 60-80% followed by the deposition and selenization of a complementary Cu-In (rich) layer. This process was found to improve the adhesion of selenized films. Hence a two-stage selenization process was standardized. In this process $Cu_{0.85}In_{0.25}$ was deposited followed by preheating in vacuum to 90° C. Copper and Cu-Ga depositions were carried out by magnetron sputtering followed by indium sputter deposition. Samples were pre-heated "in situ" so as to promote intermixing of precursors. The samples were placed in the selenization chamber for selenization. It was found that the adhesion improved and there was less globule formation of indium. This also gave an indication that a copper rich layer was required to reduce the peeling-off of the film. In the non-toxic selenization using selenium vapor, the indium loss seems to be negligible. Preliminary results indicate that the loss of gallium may be considerable during the selenization of an intermixed Cu-Ga layer. This needs to be studied further.

With the introduction of gallium into the structure the composition of $CuInSe_2$ was altered to $CuIn_{1-x}Ga_xSe_2$ (x=0.2-0.25). Calculations were carried out to estimate the thickness and the time taken for the deposition. As discussed earlier the deposition was divided into two steps. The composition in this case was $Cu_{0.85}In_{1-x}Ga_xSe_2$. In this process initially 80% of Cu-Ga was deposited on molybdenum followed by 25% of In and then 10% of Cu-Ga. This 10% of Cu-Ga was intended to avoid the globule formation of indium and indium-gallium. Copper rich layer was expected to lead to a large grain size, high conductivity and low contact resistance. Gallium was always found to diffuse towards the back contact possibly due to the stress in the Mo film

and the stress near molybdenum-copper indium selenide interface. Initially, the selenizations were carried out at 450° C. However, it was found that a higher temperature of 550° C is essential for improving the properties of the thin films and solar cells.

The novel two-selenization process developed for achieving recrystallization of Cu-rich precursor during the first selenization and conversion of Cu_xSe phase at the surfaces and grain boundaries during the second selenization of Cu-poor precursor achieved compact, large-grain microstructure. It also has improved the adhesion to Mo back-contact layer considerably. Experiments carried out to increase the bandgap by adding gallium to form selenized $CuIn_{1-x}Ga_xSe_2$ thin films with $x \approx 0.2$-0.25 also improved film adhesion still further. It may be remembered that earlier Ga_2Se_3 at the $Mo\backslash CuIn_{1-x}Ga_xSe_2$ interface has been utilized to improve adhesion [37,38]. The combination of two-selenization process and Ga addition near Mo contact have virtually eliminated the vexing problem of peeling off. Using the two selenization process, well-adherent $CuIn_{1-x}Ga_xSe_2$ thin films free from pin-holes are being prepared routinely.

Estimates of composition were made by measuring the resistance of selenized $CuInSe_2$ and $CuIn_{1-x}Ga_xSe_2$ thin films. It is known that copper rich $CuInSe_2$ and $CuIn_{1-x}Ga_xSe_2$ are highly conducting while copper-poor $CuInSe_2$ and $CuIn_{1-x}Ga_xSe_2$ films are resistive, higher the copper deficiency, higher being the resistance. Typically $Cu_{0.95}In_{1.0}Se_2$ films are known to show a resistance of several hundred KΩ across the film or molybdenum contact. Hence in the absence of composition information from other techniques, resistance measurement, together with weight by microbalance were used to adjust the composition. The calculation of the different compositions are given below:

Experiment 1

This calculation was done to find the fraction of gallium and indium in the formula $Cu_{0.85}In_{1-x}Ga_xSe_2$. The structure of the cell that was developed using this composition is shown in Figure 2. Before the first selenization it was necessary to make it a copper rich layer so as to benefit from the fluxing action of $Cu_{2-x}Se$ and also to obtain a highly conductive layer near the Mo back contact. The second region is made indium rich and resistive. This two layer approach provides higher conductivity near the back contact while it also prevented whisker formation in the copper rich region. The various thin film layers of copper, gallium and indium were deposited using the optimized pressure and power conditions.

Experiment 2

In the next set of experiments the composition was the same $Cu_{0.85}In_{0.778}Ga_{0.222}Se_2$. As shown in Figure 3, initially 90% of copper-gallium was deposited, followed by 25% indium and then selenized at a temperature of 500-550° C. During the second selenization the temperature was adjusted to about 450° C.

Experiment 3

After optimizing the selenization temperature the copper content was increased and calculation was done to find the fraction of gallium and indium in the formula $Cu_{0.90}In_{0.76}Ga_{0.24}Se_2$.

From figure 4 it can be inferred that the composition of indium was reduced. XPS depth profiling showed the atomic concentration of copper after 30 minutes was 12.08 at%, while after about 300 minutes the atomic concentration of copper was found to increase to about 14.98 at%. The atomic concentration of indium and selenium remained fairly constant. The electron probe microanalysis study done on a sample of composition $Cu_{0.85}In_{0.778}Ga_{0.222}Se_2$ showed the average composition to be Cu:In:Ga:Se to be 19.34:27.64:1.25:51.77. From both the analysis it can be inferred that the copper content was less when compared to the sum of the amounts of indium and gallium. The copper composition of 19.34% was less than the expected value of 22-24%. Indium loss was negligible, while a 10% loss of indium was expected. Thus the calibration was off. Hence the composition was modified.

Experiment 4

In the next series (Figure 5) the composition was adjusted based on the EPMA results.
Final Composition: $Cu_{0.95}In_{1-x}Ga_{1-x}Se_2 = Cu_{0.95}In_{0.75}Ga_{0.25}Se_2$. During the two stage selenization process the temperature reached a high of about 550° C. It was found that these films had low resistance values as the composition of copper was increased. At the top a discontinuous copper gallium layer was formed.

Experiment 5

Further refinement was done to obtain a continuous top Cu-Ga layer. The total thickness of copper gallium was increased to 3682.14 Å, while that of indium was decreased to 3923.64 Å. The structure of $CuIn_{1-x}Ga_xSe_2$ is shown in figure 6. During selenization the sample was subjected to a temperature of 550° C. It was found that the resistance of these samples were reduced to about 50 kΩ.

Experiment 6

In this case the same composition was maintained as above, but the precursor layers were not subjected to any preheating. This was done to see if there was a difference in the morphology of the film and also to prevent microglobule formation. From the electron probe microanalysis the composition was found to be Cu:In:Ga:Se of 22.95:25.03:1.40:50.63. This was closer to the desired composition of $Cu_{0.95}In_{0.75}Ga_{0.25}Se_2$, especially the proportion of (at.% Cu)/(at.% In + at. % Ga) was approximately 0.0.87. It was also found that the resistance was reduced to about 50-80 KΩ. This further confirmed that there is no loss of indium.

Morphology of precursors and $CuIn_{1-x}Ga_xSe_2$ thin films was studied by atomic force microscopy (AFM) because of their effect on photovoltaic properties of solar cells. Very small sub-grain

features were studied for the *first time* by AFM, and quantitative data on rms roughness and size distribution, and 3-d images were obtained [36]. The various metallic layers and two-selenization process sequence is shown in figure 5. The metallic layer of the alloy Cu-Ga(22 at.%) was found to be very smooth with rms roughness of only 8.8 Å. 3-d image in figure 7 shows smoothly undulating surface of the film deposited on a Si\$SiO_2$ substrate. Figures 8 and 9 show 3-d AFM images of samples consisting of a 2209 Å thick Cu-Ga alloy layer, followed by 981 Å thick In and 736 Å thick Cu-Ga deposited respectively on Si\$SiO_2$ and glass\Mo substrates. Both the samples were heat-treated *in situ* at 80° C for 10 min in vacuum, prior to removal from the chamber. Formation of isolated hillock-peaks can be seen in the sample deposited on Si\$SiO_2$ substrate. On the other hand, the film on the glass\Mo substrate consists of more contiguous and rounded hillocks. Corresponding histograms in figures 10 and 11 show a more peaked distribution in the case of the film on Si\$SiO_2$ substrate. The difference in the morphology may be attributed to the higher difference of free surface energies between the film and the substrate in the case of the sample on Si\$SiO_2$. The surface energy of In is high. This usually leads to the formation of 3-dimensional islands. In the deposition of several materials such as chromium a continuous film is obtained at a thickness of ~450 Å. However low-melting-point materials such as In may require much higher thickness. A weak subgrain structure can be discerned at higher magnifications, most probably because of the secondary nucleation and tendency towards globule formation of In deposits (Fig. 12).

The first selenization at 550° C of the glass\Mo\Cu-In-Ga sample resulted in a weakly faceted growth of well-connected hillocks (Fig. 13). The film is more continuous and that there are very few voids present. The surface energy of the selenized areas is probably lower allowing more uniform coverage of the surface. In some of the selenizations, the subgrain structure seems to disappear completely after the first selenization. The subgrain structure can be seen to reappear when the second metallization layers consisting of 2943 Å In followed by 736 Å of Cu-Ga alloy are deposited (Fig. 14). The subgrain structure can be seen to disappear completely after the second selenization at 550° C. Homogenization of the metallic precursor by *in situ* preheat-treatment at ~80-90° C prior to the first selenization, the selenization temperature, and the rate of selenium evaporation play important roles in determining the structure and morphology of $CuIn_{1-x}Ga_xSe_2$ thin films. AFM images of good quality $CuIn_{1-x}Ga_xSe_2$ samples show large, compact, well-faceted grains with crystallographic shapes (Fig. 15). The most stable growth form of chalcogenides is known to correspond to the polyhedron, which is visible in many of the grains. The anisotropy of the $[112]_{Me}$ and $[112]_{Se}$ direction favors, under certain conditions the growth of the plane with the higher surface energy. In this case it is the $[112]_{Se}$ directions so that the surface of the grains is formed by the $[112]_{Me}$ planes (Figure 16). The presence of some pits can also be seen. The rms roughness of the completed $CuIn_{1-x}Ga_xSe_2$ layers was in the range 950-1500 Å. The morphology of completed $CuIn_{1-x}Ga_xSe_2$ thin films was superior when the metallic precursors were pre-heated *in situ* prior to the first selenization. A selenization temperature >523° C is essential for obtaining the fluxing action of $Cu_{2-x}Se$. On the other hand, an excessively high selenization temperature especially coupled with a low selenium vapor incidence rate results in a rough morphology in parts of the film. This is seen in an AFM image from a sample the selenization temperature of which was high enough to cause softening of the glass substrate at the edges whilst the selenium vapor incidence rate was very low (<25 Å s^{-1})

(Fig. 17). The rms roughness of this sample was 1950 Å. An interruption of selenium vapor incidence also resulted in a rough morphology. An optimum temperature of 550° C is therefore, chosen for best results. The optimum value of selenium vapor incidence rate was found to be 25-50 Å s^{-1}.

Figure (18) shows the fine grain morphology of a sample which consisted of only the second set of metallic precursors Cu-In-Ga deposited on glass\Mo substrate after undergoing a selenization at 500° C.

2.1.2 Fabrication of $CuIn_{1-x}Ga_xSe_2$ Solar Cells

Several cells were completed and measured at Institute of Energy Conversion (IEC)-University of Delaware by deposition of thick CdZnS:In\ITO\Ni fingers on glass\Mo\$CuIn_{1-x}Ga_xSe_2$ samples prepared at FSEC with the near optimum atomic proportions. Solar cells prepared from $CuIn_{1-x}Ga_xSe_2$ thin films in which the precursors were not homogenized showed V_{oc} of 378 mV, J_{sc} of 33.4 mA, a fill factor of 60.2% and an active area conversion efficiency of 7.6%. The best cell obtained with films prepared using precursors homogenized *in situ* prior to selenization gave an open circuit voltage V_{oc} of 377 mV, J_{sc} of 34.8 mA, a fill factor 62.5% and active area conversion efficiency of 8.2% (Fig. 19) [39]. Spectral response was found to be fairly constant over the entire spectral range (Fig. 20). V_{oc} improved to 402 mV after 200° C heat treatment in air. However, the efficiency was reduced to 6.3%. Low values of fill factor were attributed to the 1.6-μm thick CdZnS:In heterojunction layer which also resulted in the loss of spectral response from high energy photons.

The morphology of the completed films was found to correlate well with the photovoltaic properties of the completed devices. Thus the best solar cells prepared from $CuIn_{1-x}Ga_xSe_2$ thin films in which the precursors were not homogenized showed V_{oc} of 378 mV, J_{sc} of 33.4 mA, a fill factor of 60.2% and an active area conversion efficiency of 7.6%. The best cell obtained with films prepared using precursors homogenized *in situ* prior to selenization, and thus having a superior morphology, gave an open circuit voltage V_{oc} of 377 mV, J_{sc} of 34.8 mA, a fill factor 62.5% and active area conversion efficiency of 8.2%. A much more accentuated drop in the photovoltaic properties was observed when the $CuIn_{1-x}Ga_xSe_2$ contained regions having a rough morphology either because of an excessively high selenization temperature, or a low or interrupted selenium vapor incidence rate. The complete disappearance or not of the subgrain structure after the first selenization also affected the photovoltaic properties of solar cells prepared from $CuIn_{1-x}Ga_xSe_2$ obtained after the second selenization. It was, therefore, important to carry out each of the selenizations under the optimum conditions.

A few cells were also completed at the National Renewable Energy Laboratory (NREL) by deposition of thin CBD CdS\ZnO:Al\Ni-Al grid contact on glass\Mo\$CuIn_{1-x}Ga_xSe_2$ samples prepared at FSEC. The V_{oc} of all the cells was in the 370-388 mV range. The best cell showed J_{sc} of 31.5 mA, fill factor of 45.1% and the total area efficiency of 5.87%. It may be concluded that the values of V_{oc} of 370-400 mV and of J_{sc} of ~35 mA are reasonable. It is now essential to concentrate on reducing the series resistance and increase the shunt resistance so as to improve

the conversion efficiencies.

2.2 CdTe Thin-Film Solar Cells

Most of the groups are using commercial SnO_2:F coated sodalime glass substrates for CdTe solar cells. Sodalime glass imposes limits on the maximum processing temperatures. As mentioned above, the highest efficiency (15.8%) has been achieved with cells fabricated by CSS on borosilicate glass substrates coated with high quality SnO_2:F window layers. Chemical bath deposition (CBD) technique has been well-developed at FSEC and CdS layers for CdTe solar cells are being prepared routinely from acetate reactants [40,41].

2.2.1 CdTe Absorber and Interface and Junction between CdS\CdTe

Considerable work was carried out on the magnetron-sputter deposition of Cd and Te layers, suitability of targets for sputtering of tellurium, heat treatments in various ambients such as vacuum and partial pressures of nitrogen, nitrogen-oxygen, and helium-oxygen mixtures for phase formation and grain growth. Pinhole formation and peeling off problems were frequent in initial experiments. These were traced to cleanliness of the glass\$SnO_2$:F\CdS substrates and lack of adhesion of sputtered Cd and Te layers. Cleaning and handling procedures were developed so as to improve the adhesion of and to eliminate pinholes in as-deposited layers. Magnetron sputtering of Cd did not pose problems. However, vacuum melted targets and adequate thermal and electrical contact between the magnetron sputtering source and Te target and efficient water cooling were found to be essential for well-controlled Te deposition at high deposition rates. Well-adherent Te and Cd layers are being deposited routinely on glass\$SnO_2$:F\CdS samples at high deposition rates. It is estimated that using this technique, higher and controllable deposition rates could be employed to allow deposition of elemental Cd\Te layers required to form >4 μm thick CdTe film in <4 min.

Initially a sequential approach was followed. It consisted of elemental layer deposition on unheated glass\SnO_2:F\CdS substrates, phase formation by heat treatment in an inert ambient such as vacuum or nitrogen; and grain-growth, junction-formation, and type-conversion by $CdCl_2$ treatment in air or helium-oxygen mixture at ~400° C. Experiments were carried out with combinations of Te first, Cd first, Te last, and Cd last stacking sequences of Cd\Te elemental stacks. Adhesion problems were least for Te first sequence because of better adhesion of Te layers to the substrate. A Te layer at the top was found to minimize Cd reevaporation. Hence all the subsequent elemental stacks consisted of first and last Te layers. A first Te layer would probably play a beneficial role in promoting the growth of mixed $CdS_{1-x}Te_x$ and CdS_yTe_{1-y} interface layers.

Initially stoichiometric Cd/Te were deposited. Later experiments were conducted with excesses of Cd or Te. Thicknesses of Cd/Te layers deposited on glass\SnO_2:F\CdS substrates were varied to obtain compositions ranging from 10% Cd-rich to 30% Te-rich. X-ray diffraction (XRD) analysis of samples heat-treated at <300° C for 30 minutes showed complete CdTe phase formation with traces of CdO, and TeO_3 (Figure 21). X-ray photoelectron spectroscopy (XPS)

is a very powerful technique for analyzing CdTe thin films especially because it can provide information on the chemical states of tellurium. XPS analysis showed the presence of traces of CdTe even in as-deposited Cd\Te layers on unheated substrates. Complete CdTe phase formation was observed by XRD and XPS analysis after heat treatment at temperatures <300° C for 30 minutes of Cd/Te elemental layers with a small excess Cd or Te. As can be seen in the figure 22, there is a measurable shifts in the XPS peaks Te $3d_{3/2}$ and $3d_{5/2}$ incorporated as CdTe, and incorporated in TeO_x. XPS analysis of Cd-rich as well as Te-rich Cd/Te layers heat-treated at temperatures <300° C in 300 Torr N_2 showed mostly the presence of Te incorporated in the CdTe phase. Most of the tellurium oxide was near the surface region. Figure 23 shows the XPS spectra of heat-treated CdTe sample, the green curve corresponding to the surface (0 min etch) and the red curve corresponding to sample etched for 10 min. It can be seen that near the surface of the sample, Te incorporated as TeO_x was higher than that incorporated as the CdTe phase. After a 10 minute sputter-etch with argon ions, CdTe became the predominant phase, thus the bulk of the film consisted mostly of CdTe. $CdCl_2$ treatment, consisting of spreading drops of $CdCl_2$:methanol solution on the sample surface and heat-treatment at 350-450° C for 30 minutes in air or nitrogen-oxygen mixtures was carried out to improve the grain size. XPS analysis showed that CdTe was again the primary phase in samples consisting of Cd/Te layers on glass\SnO_2:F substrates and which were coated with $CdCl_2$ and heated in air at 400° C for 30 minutes. Small Te excesses in the precursors is known to promote p-type conductivity in completed CdTe layers. Hence all the subsequent experimentation was carried out with small excesses of Te.

Grain size improved with increasing heat-treatment temperature. In the initial experiments, pinholes were observed for temperatures of heat treatments approaching 400° C. Hence attempts were made to carry out the phase formation at temperatures of 320-390° C. These films showed poor junction formation on $CdCl_2$ treatment at 400° C.

Later a new integrated approach was followed. The emphasis was shifted from CdTe phase formation to CdS\CdTe interface and junction formation by heat treatments at 450-475° C since CdTe phase formation occurs easily at temperatures of ~300° C. Excessive problems of peeling-off and pinhole formation were encountered for heat treatments at temperatures >440° C especially in the case of samples having thin (<1500 Å) CBD grown CdS layers. XPS analysis of substrates and back sides of peeled-off films revealed the presence of carbon, most probably because of diffusion to the interface of backstreaming mechanical-vacuum-pump-fluid vapor (Figure 24). This problem was corrected. In some cases, fluorine possibly out-diffusing from SnO_2:F window layer was detected at the back of the peeled off CdTe films especially when the CdS layer had undergone a high temperature processing (Figure 25). This phenomenon needs to be studied further. Special emphasis was placed on obtaining thicker CBD grown CdS layers. Some 3000-6000 Å thick CdS layers were kindly provided by Solar Cells Inc (SCI). Special precautions were taken to assure that contaminants were not introduced on to the glass\SnO_2:F\CdS samples during the handling or from the laboratory glassware. Thicker CdS layers either grown by CBD or supplied by SCI were employed in all the subsequent experiments to assure interface and junction formation at high temperatures without excessive problems of peeling-off and pinholes. Excessive reevaporation of Cd and even Te at temperatures over 440°

C was found to lead to pinhole formation. A semi-closed graphite crucible and 5-30% Te excess with a Te top layer were found to minimize reevaporation.

In some of the experiments, $CdCl_2$ was applied to glass\$SnO_2$:F\CdS samples by immersing in $CdCl_2$-methanol solution or by placing its drops, and also by vacuum evaporation [28]. Laser evaporation of $CdCl_2$ has also been used successfully [42]. Peeling off problems were frequent in heat treatment of Cd/Te elemental stack deposited on $CdCl_2$-coated glass\$SnO_2$:F\CdS samples especially because of the hygroscopic nature of $CdCl_2$ and the exposure to the atmospheric humidity during specimen transfer from one chamber to the other. Peeling off problems were considerably reduced when $CdCl_2$ was applied on to Cd/Te stacks on glass\$SnO_2$:F\CdS samples.

Tellurium oxide and cadmium chloride were detected by XPS analysis at considerable depths in the $CdCl_2$-treated Te-rich samples and heated in oxygen-containing ambients at 350-450° C. The oxide layers in these samples had not been removed by etching in acidic solutions.

After eliminating the various causes of pinhole formation and peeling off, it became possible to identify the effect of heat-treatment ambients viz. vacuum, nitrogen, and oxygen:inert gas mixtures on the peeling off and pinhole formation especially at higher temperatures. Based on empirical observations, the heat treatment ambients were optimized. Finally this has made it possible to routinely prepare well-adherent and mostly pinhole-free CdTe layers on glass\SnO_2:F\CdS samples. These films are considerably robust as compared to CdTe films deposited by other low-temperature processes.

2.2.2 Fabrication of CdTe Solar Cells

Prior to solar cell completion, all the samples were coated with $CdCl_2$ mostly by immersion in $CdCl_2$:methanol solution and were heated at 400° C for 30 minutes in $He:O_2$ 80:20 mixture. The oxide layers were then removed by etching the samples in $H_3PO_3:HNO_3:H_2O$ acidic solution. Solar cells were prepared by applying doped graphite paste, and silver paste contacts. Some of the cell completion was carried out at NREL. CdTe thin-films Solar cells prepared after low-temperature (≤400° C) heat-treatments described above showed V_{oc} of 320-380 mV, J_{sc} of ~5 mA and a poor FF values of ~30%. Open circuit voltage values above 580 mV have been obtained in the case of cells using high-temperature treated CdTe layers prepared from $CdCl_2$ coated Cd/Te stacks. Most probably the low short-circuit current and poor fill factor values result from blocking contacts or junction formation away from the CdTe\CdS interface.

Cd, Te, high temperature (~450° C), oxygen, and $CdCl_2$ are the essential ingredients in the preparation of CdTe thin film solar cells on glass\$SnO_2$:F\CdS samples [11,17,28,33]. Adequate understanding, careful process optimization in the preparation of each layer as well as and proper control of the processing steps is essential so as to obtain well-adherent and fairly pin-hole free CdTe layers with thicknesses in the range 4-6 μm. FSEC has developed a base-line process which includes all the above ingredients for the routine preparation of well-adherent 4-6 μm CdTe thin films on glass\$SnO_2$:F\CdS samples. A junction formation has been observed. The open-circuit voltage V_{oc} values are approaching 600 mV. Unfortunately, as discussed earlier,

providing all the essential ingredients does not necessarily result in high-efficiencies. A blocking contact and especially the formation of a junction away from the CdTe\CdS interface often have been found to result in low efficiencies [28,31]. The standard recipes developed for obtaining high efficiency solar cells from several of the other processes can only serve as guidelines. It is now essential to develop an optimum process for improving the short-circuit current and fill factor values by eliminating any blocking contacts and avoiding junction formation away from the CdTe\CdS interface, and thus to achieve highly efficient CdTe thin-film solar cells by using the promising approach of using Cd/Te layers.

The hygroscopic nature of $CdCl_2$ and the high humidity in Florida make it difficult to obtain the maximum benefit from the $CdCl_2$ treatment. Moreover, the present 6"-six-way cross type of chamber utilized for magnetron sputtering of Cd and Te elemental layers places considerable constraints on the experimental set-up. Hence it is planned to install a new vacuum deposition system with large (18" dia.) chamber pumped with a cryopump to obtain clean vacuum, free from hydrocarbon and water vapors. The new chamber is expected to provide more flexibility in optimizing the deposition of Cd\Te layers, application of vacuum evaporated $CdCl_2$, and processing of the samples.

3. CONCLUSIONS

FSEC has established a well-equipped laboratory with hazardous material handling capabilities for research and development on thin-film solar cells. Gallium-indium form a low temperature eutectic with the eutectic point at ~17° C. Indium-gallium or gallium layers would invariably result in liquid or liquid-like behavior destroying the structural stability. A new process being developed at FSEC can solve the problem of incorporation of gallium without encountering the deleterious interaction between indium and gallium. In this process, the difficulty of low-melting point precursors has been avoided by incorporating gallium using a single Cu-Ga(22 at.%) alloy target. Internal stresses in refractory metal Mo films were minimized by employing higher working gas pressure to moderate the flux and energy of these particles. Magnetron-sputter-depositions of Mo and Cu-In-Ga metallic precursor films were carried out in a 18" diameter and 24" height bell jar. Cd and Te layers were magnetron-sputtered in a 6-way 6" diameter cross type chamber pumped with a turbomolecular pump. The Cu/In films were subjected to a *in situ* heat treatment at 80-90° C for 10 min. A novel two-selenization process using Se vapor has been developed for achieving recrystallization of Cu-rich precursor during the first selenization and conversion of $Cu_{2-x}Se$ phase at the surfaces and grain boundaries during the second selenization of Cu-poor precursor. A higher selenization temperature of 550° C was found to be essential for improving the properties of the thin films and solar cells. The novel two-selenization process improved the adhesion to Mo back-contact layer considerably. Experiments carried out to increase the bandgap by adding gallium to form selenized $CuIn_{1-x}Ga_xSe_2$ thin films with $x \approx 0.2$-0.25 also improved film adhesion still further. The combination of two-selenization process and Ga addition near Mo contact have virtually eliminated the vexing problem of peeling off.

A series of experiments were carried out to obtain the desired composition and a compact, large-grain microstructure. EPMA analysis showed the composition to be closer to the desired composition of Cu:In:Ga:Se of 22.95:25.03:1.40:50.63. Morphology of precursors and $CuIn_{1-x}Ga_xSe_2$ thin films was studied because of their effect on photovoltaic properties of solar cells. Very small sub-grain features were studied for the *first time* by atomic force microscopy, and quantitative data on rms roughness and 3-d images were obtained. Several cells were completed and measured at IEC. The best cell obtained with films prepared using precursors homogenized *in situ* prior to selenization gave an open circuit voltage V_{oc} of 377 Mv, J_{sc} of 34.8 Ma, a fill factor 62.5% and active area conversion efficiency of 8.2%. Spectral response was found to be fairly constant over the entire spectral range. A few cells were also completed at NREL. Best J_{sc} of 31.5 mA, fill factor of 45.1%, V_{oc} of 370-388 mV, and the total area efficiency of 5.87% were measured.

Chemical bath deposition technique has been well-developed at FSEC and CdS layers for CdTe solar cells are being prepared routinely from acetate reactants. Considerable work was carried out on the magnetron-sputter deposition of Cd and Te layers, suitability of targets for sputtering of tellurium, heat treatments in various ambients for phase formation and grain growth. Elemental stacks consisted of first and last Te layers so as to obtain better adhesion and to minimize Cd reevaporation. Most experiments were carried out with small excesses of Te to promote p-type conductivity. Complete CdTe phase formation was observed by XRD and XPS analysis after heat treatment at temperatures <300° C for 30 minutes of Cd/Te elemental layers with a small excess Cd or Te. CdS\CdTe interface and junction formation was promoted by heat treatments at 450-475° C. Excessive problems of peeling-off and pinhole formation encountered for heat treatments at temperatures >440° C were resolved by using thicker CdS layers. A semi-closed graphite crucible and 5-30% Te excess with a Te top layer were used to minimize Cd and even Te reevaporation at temperatures over 440° C. Peeling off problems were frequent in heat treatment of Cd/Te elemental stack deposited on $CdCl_2$-coated glass\$SnO_2$:F\CdS samples especially because of the hygroscopic nature of $CdCl_2$. Peeling off problems were considerably reduced when $CdCl_2$ was applied on to Cd/Te stacks on glass\$SnO_2$:F\CdS samples. Well-adherent and mostly pinhole-free CdTe layers on glass\$SnO_2$:F\CdS samples are being prepared routinely. Completed CdTe cells prepared after low-temperature (≤400° C) heat-treatments showed V_{oc} of 320-380 mV, J_{sc} of ~5 mA and a poor FF values of ~30%. Solar cells prepared using high-temperature-treated CdTe layers showed V_{oc} of >580 mV, however with low J_{sc} and poor fill factor values most probably resulting from blocking contacts or junction formation away from the CdTe\CdS interface.

4. ACKNOWLEDGEMENTS

We would like to sincerely thank Dr. Bolko von Roedern, Dr. Harin S. Ullal, Ken Zweibel, Dr. Kannan Ramanathan, Ramesh G. Dhere, Helio R. Moutinho, and Dr. Dave Albin of NREL, Dr. Robert Birkmire, IEC, Dr. Peter Meyer of Solar Cells Inc., Dr. Robert Gay of Siemens Solar Ind., Dr. Rajeewa Arya of Solarex Corp., Dr. Alan E. Delahoy of Energy Photovoltaics Inc., Dr.

Michele Migliuolo of Kurt J. Lesker Co., and Dr. Peter F. Gerhadinger of Libbey Owens Ford for many useful discussions. We would also like to gratefully acknowledge the help of Dr. Peter Meyer, Solar Cells Inc. in providing glass\$SnO_2$:F\CdS samples, Dr. Peter F. Gerhadinger, Libbey Owens Ford in providing glass\$SnO_2$:F samples, Dr. Robert Gay, Siemens Solar Ind. and Dr. Rajeeva Arya, Solarex Corp. in providing glass\Mo samples, Dr. Kannan Ramanathan and Ramesh G. Dhere in completion of CdTe solar cells, Dr. Robert Birkmire and Dr. Kannan Ramanathan in the completion of $Cu(In_{1-x}Ga_x)Se_2$ thin-film solar cells, Alice Mason of NREL in EPMA analysis, Helio R. Moutinho of NREL in AFM analysis, Dr. Orlando Melendez in XPS analysis, and Dr. Bijoy K. Patnaik and Dr. Nalin R. Parikh in RBS and PIXE analysis; and Dr. Michele Migliuolo, Kurt J. Lesker Co. for donation of two magnetron sputtering sources and Martin Marietta Missiles Co. for donation of an old vacuum system.

5. REFERENCES

1. H. Ullal, K. Zweibel, and B. G. von Roedern, Proc. ISES Solar World Congress, Budapest, Hungary, Aug. 23-27, 1993.
2. N. G. Dhere, Recent Developments in Thin-Film Solar Cells, Thin Solid Films 194, (1990), p. 757.
3. A. M. Gabor, J. R. Tuttle, D. S. Albin, M. A. Contreras, and R. Noufi, To be published in J. Appl. Phys.
4. T. Walter and H. W. Schock, Thin Solid Films 224, (1993), p. 74.
5. D. Bonnet, Int. J. Solar Energy, 12, (1992), p. 1.
6. T. L. Chu, and S. S. Chu, Progress in Photovoltaics: Res. & Appl., 1, (1993), p. 31.
7. R. H. Bube and K. W. Mitchell, J. Ele. Materials, 22, No. 1, (1993), p. 70.
8. L. Skarp, E. Antilla, A. Rautiainen, and T. Suntola, Int. J. Solar Energy, 12, (1992), p. 137.
9. C. Ferekides, J. Britt, L. Killian, Proc. 23rd IEEE Photovoltaic Specialists' Conference, Louisville, KY, May 10-14, 1993, p. 389.
10. S. Ikegami, Solar Cells, 23, (1988), p. 89.
11. B. M. Başol, Solar Cells, 23, (1988), p. 69.
12. R. Gay, M. Dietrich, C. Fredric, C. Jensen, K. Knapp, D. Tarrant, D. Willet, Presented at 12th European Photovoltaic Solar Energy Conference, Amsterdam, in April 1994.
13. V. K. Kapur, B. M. Başol, A. Halani, C. R. Leidhlm, and A. Minnick, Presented at 12th EPVSEC, Amsterdam, in April 1994.
14. A. Delahoy, J. Britt, G. Butler, F. Faras, A. Sizemore, F. Ziobro, and Z. Kiss, Presented at 12th EPVSEC, Amsterdam, in April 1994.
15. J. F. Jordan and S. P. Albright, Solar Cells, 23, (1988), p. 107.
16. P. V. Meyers, T. Zhou, R. C. Powell, and N. Reiter, Proc. 23rd IEEE PVSC, Louisville, KY, May 10-14, 1993, p. 400.
17. J. M. Woodcock, M. E. Özsan, A. K. Turner, D. W. Cunningham, D. R. Johnson, R. J. Marshall, N. B. Mason, S. Oktik, M. H. Patterson, S. J. Ransome, S. Roberts, M. Sadeghi, J. M. Sherborne, D. Sivapathasundaram, I. A. Walls, Presented at 12th EPVSEC, Amsterdam, in April 1994.

18. P. D. Moskowitz and K. Zweibel (eds), "Recycling of Cadmium and Selenium from photovoltaic modules and manufacturing waste: A workshop Report", Brookhaven National Laboratory, Report No. 47787.
19. M. H. Patterson, A. K. Turner, M. Sadeghi, and R. J. Marshall, Presented at 12th EPVSEC, Amsterdam, in April 1994.
20. R. Klenk, R. Menner, D. cahen, and H. W. Schock, Proc. 21st IEEE PVSC, Kissimimmee, FL, 1990, p. 481.
21. T. J. Vink, M. A. J. Somers, J. L. C. Daams, and A.G. Dirks, J. Appl. Phys., 70, (1991), p. 4301.
22. J. Szot and U. Prinz, J. Appl. Phys., 66, (1989), p. ..
23. R. A. Sasala, X.X. Liu, and J. R. Sites, Int. J. Solar Energy, 12, (1992), p. 17.
24. J. L. Pautrat, J. M. Francou, N. Magnea, E. Molva, and K. Saminadayar, J. Crystal Growth, 72, (1985), pp. 194-204.
25. J. A. Van Vechten, J. D. Zook, R. D. Horning, and B. Goldenberg, Jpn. J. Appl. Phys., 31, (1992), p. 3662.
26. R. M. Park, M. B. Troffer, C. M. Rouleau, J. M. DePuydt, and M. A. Haase, Appl. Phys. Lett., 57, (1990), p. 2127
27. Y. S. Tyan, Solar Cells, 23, (1988), p. 19.
28. B. M. Başol, Int. J. Solar Energy, 12, (1992), p. 25.
29. R. W. Birkmeyer, B. E. McCandless, and W. N. Shafarman, Solar Cells, 23, (1988), p. 23.
30. R. W. Birkmeyer, B. E. McCandless, and S. S. Hegedus, Int. J. Solar Energy, 12, (1992), p. 145.
31. A. Rohatgi, 23rd IEEE PVSC, Louisville, KY, May 10-14, 1993, p. 481.
32. M. E. Özsan, D. R. Johnson, D. W. Lane, and K. D. Rogers, Presented at 12th EPVSEC, Amsterdam, in April 1994.
33. M. T. Bhatti, K. M. Hynes, R. W. Miles, and R. Hill, Int. J. Solar Energy, 12, (1992), p. 171.
34. Glang and Maissel
35. J. Kessler, D. Schmid, S. Zweigart, and H. W. Schock, Proc.23rd IEEE PVSC.(1993),p. 549.
36. R. Klenk, T. Walter, D. Schmid, and H. W. Schock, Proc. Int. Conf. on Ternary and Multinary Compounds, Yokohama, Japan, Aug. 8-12, 1993.
37. N. G. Dhere, S. Kuttath, and H. R. Moutinho, accepted for presentation at the 41st National Symposium of the American Vacuum Society to be held at the Colorado Convention Center, Denver, CO, during Oct. 24-28, 1994.
38. G. Pollock, K. Mitchell, J. Ermer, European Patent No 0 360 403 A2 (1989).
39. N. G. Dhere, D. L. Waterhouse, K. B. Sundaram, O. Melendez, N. R. Parikh, and B. K. Patnaik, accepted for publication in J. Materials Science: Materials in Electronics.
40. N. G. Dhere and S. Kuttath, submited for presentation at the First World Conference on Photovoltaic Energy Conversion to be held at Waikoloa, Hawaii during Dec. 5-9, 1994.
41. N. G. Dhere, D. L. Waterhouse, K. B. Sundaram, O. Melendez, N. R. Parikh, and B. K. Patnaik, Proc. 23rd IEEE PVSC, Louisville, KY, May 10-14, 1993, p. 566.
42. A. Compaan and A. Bhat, Int. J. Solar Energy, 12, (1992), p. 155

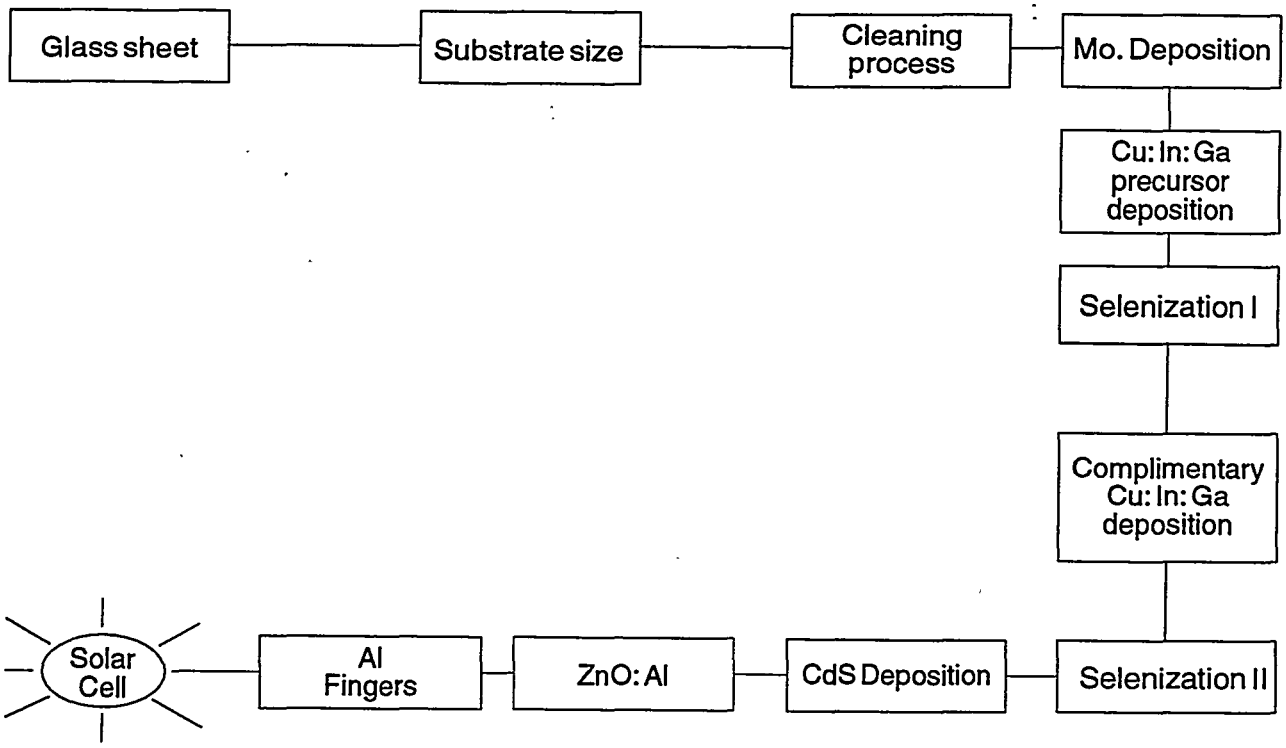

Fig. 1. Process chart an overall view of the entire process that leads to the fabrication of a $CuIn_{1-x}Ga_xSe_2$

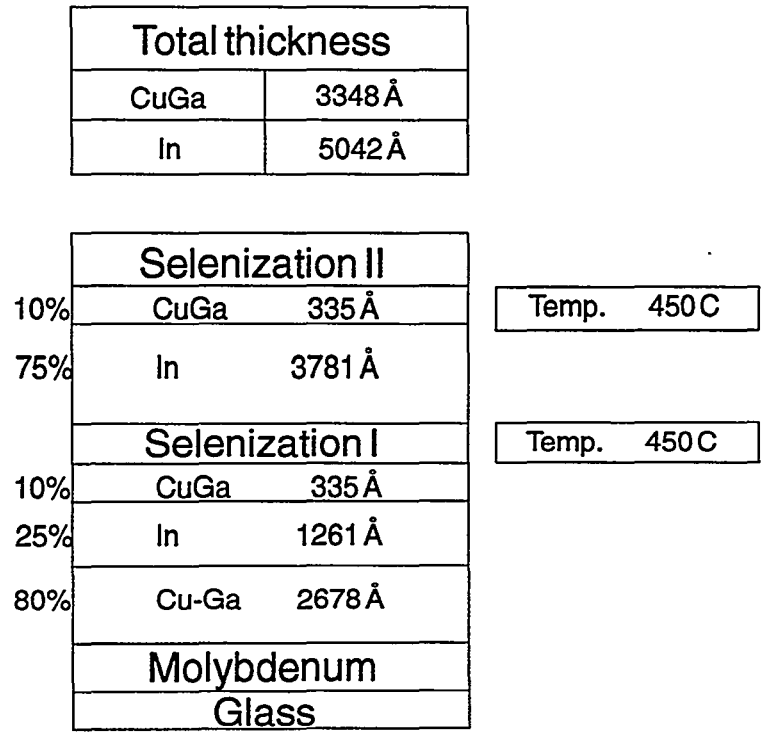

Fig. 2. Schematic layout of $Cu_{0.85}In_{1-x}Ga_xSe_2$

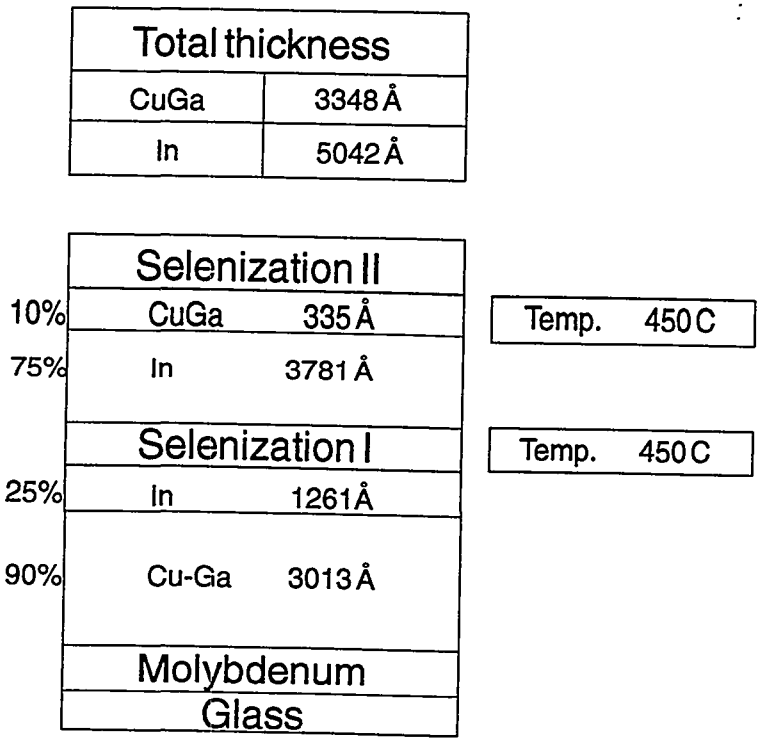

Fig. 3. Schematic layout of $Cu_{0.85}In_{0.778}Ga_{0.222}Se_2$

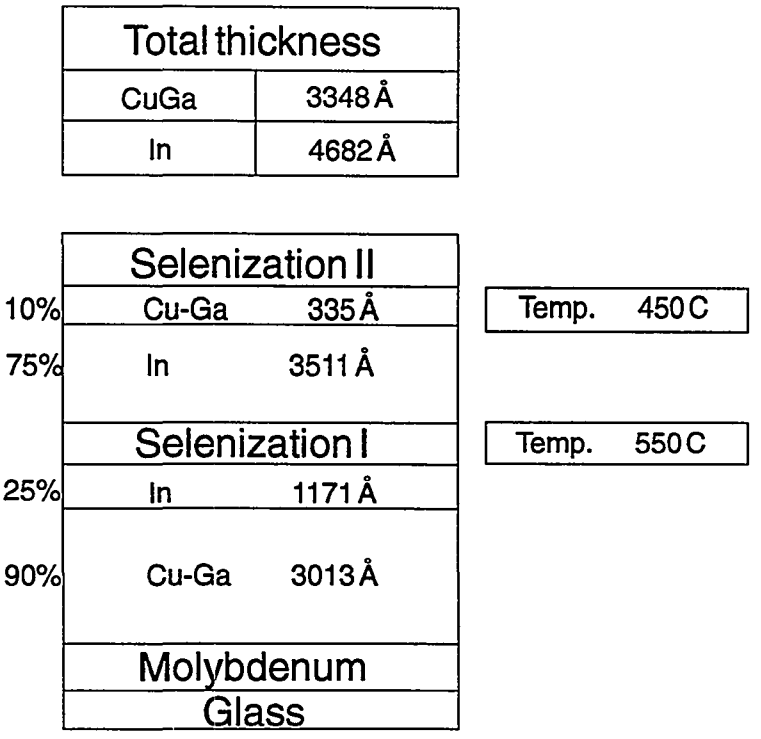

Fig. 4. Schematic layout of $Cu_{0.90}In_{0.76}Ga_{0.24}Se_2$

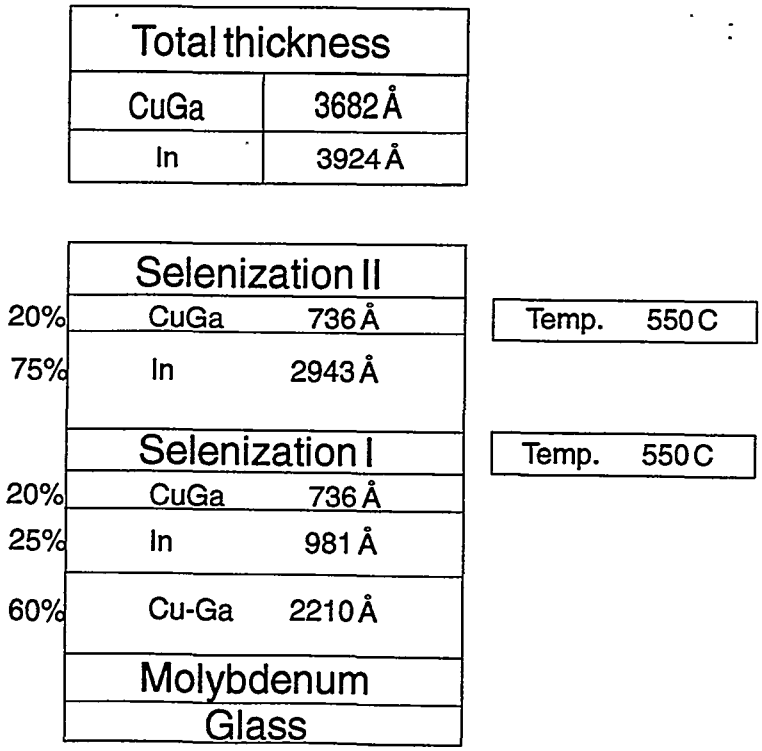

Fig. 5. Schematic layout of $Cu_{0.95}In_{0.75}Ga_{0.25}Se_2$

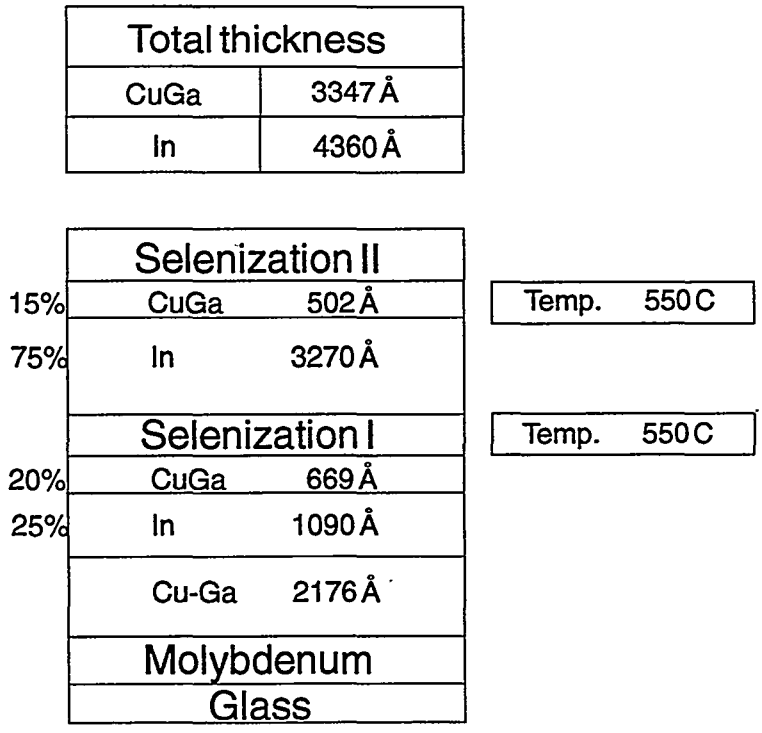

Fig. 6. Schematic layout of $Cu_{0.95}In_{1-x}Ga_xSe_2$

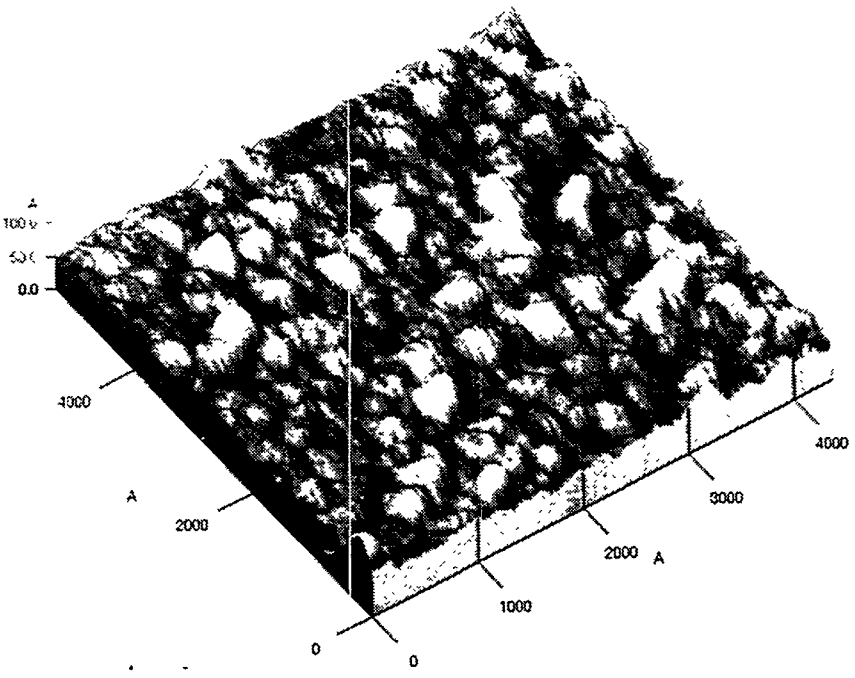

Figure 7. Image of smoothly undulating surface of the film deposited on a Si/SiO_2 substrate

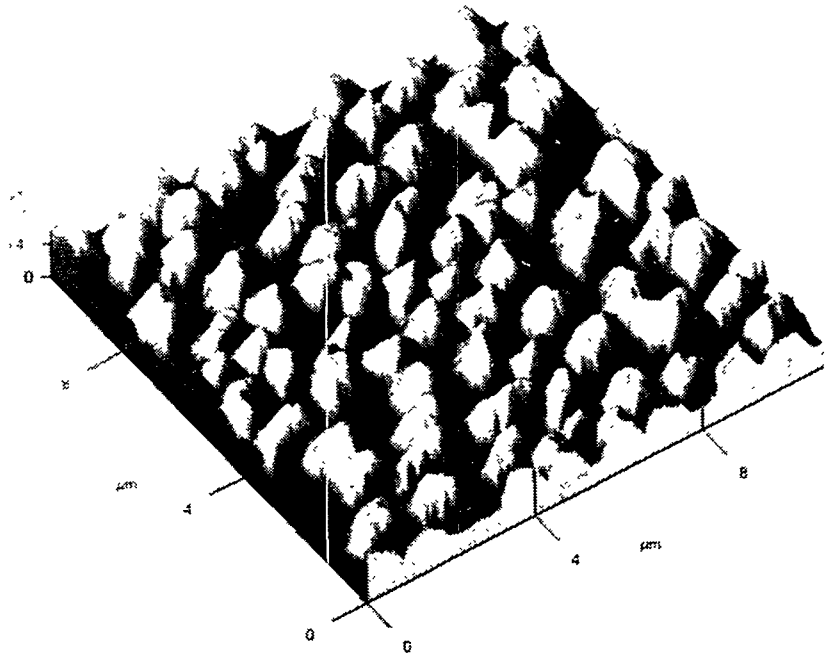

Figure 8. 3-D AFM images of samples consisting of a 2209 Å Cu-Ga + 981 Å In + 736 Å Cu-Ga deposited on Si/SiO_2 substrates

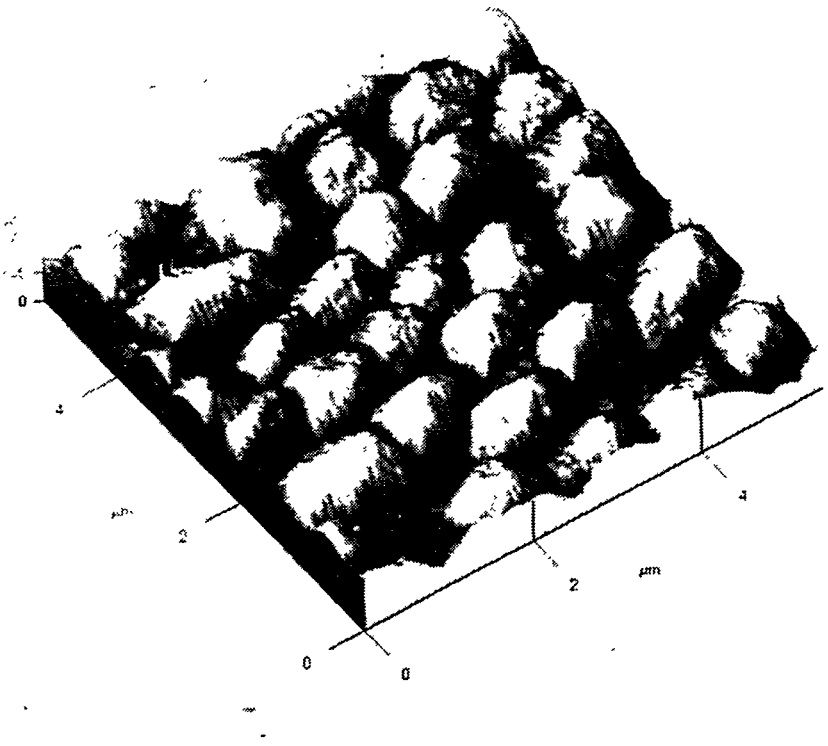

Figure 9. 3-D AFM images of samples consisting of a 2209 Å Cu-Ga + 981 Å In + 736 Å Cu-Ga deposited on glass/Mo substrates

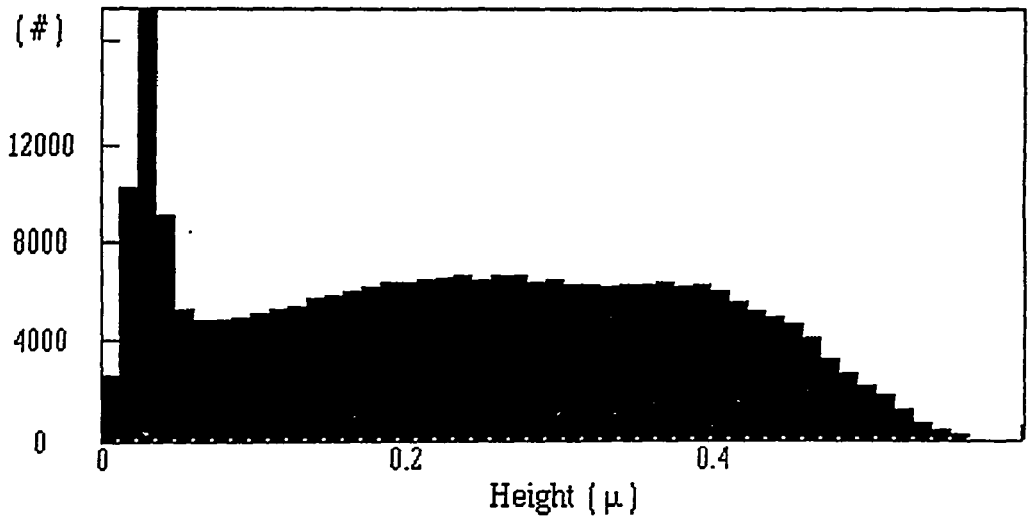

Figure 10. Histogram of the size distribution of sample in Figure 8

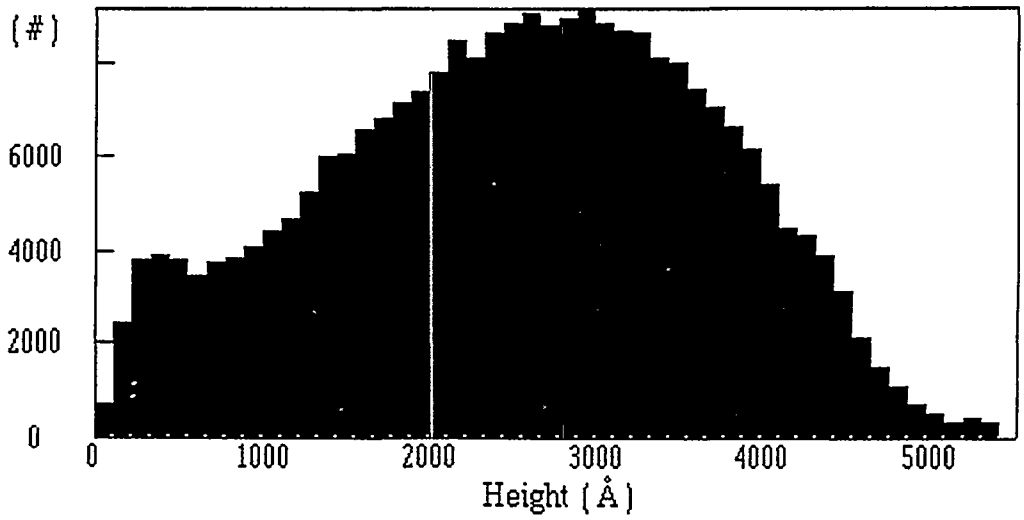

Figure 11. Histogram of the size distribution of sample in Figure 9

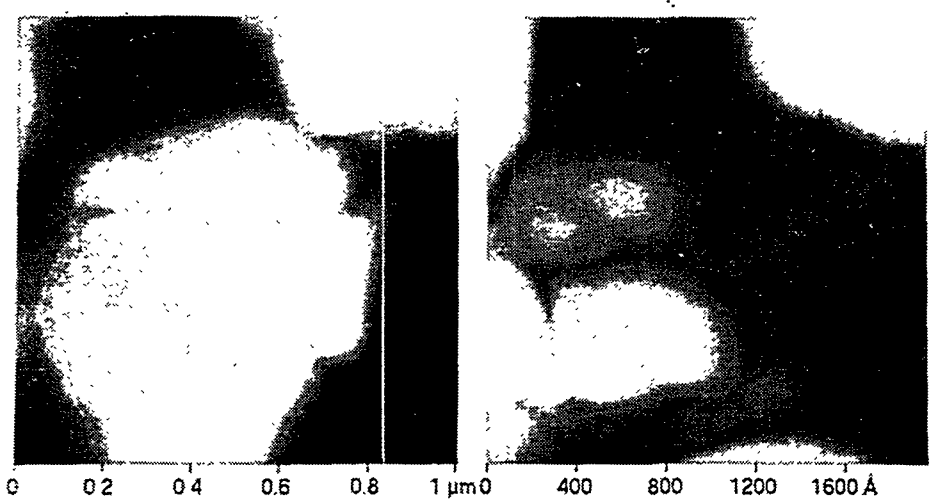

Figure 12. 2-D AFM image of the sample in Figure 9 showing weak subgrain structure at higher magnifications

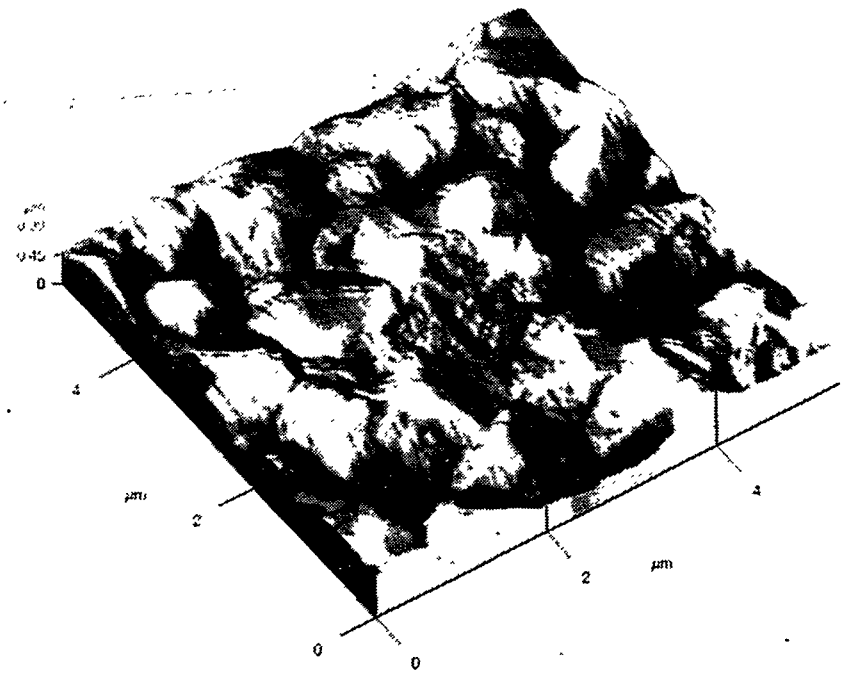

Figure 13. 3-D AFM image after the first selenization at 550°C of the glass/Mo/Cu-In-Ga sample

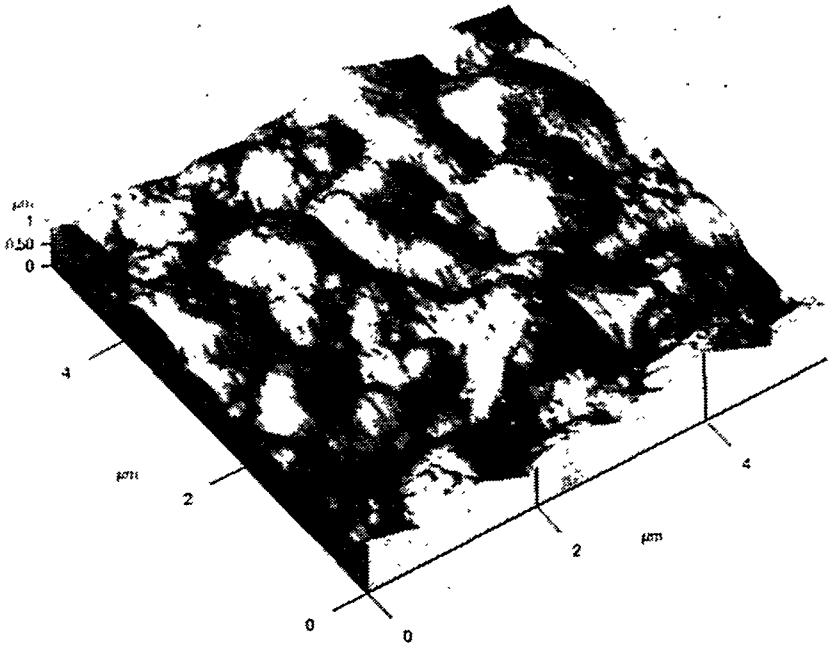

Figure 14. 3-D AFM image showing the reappearance after the second metallization layers

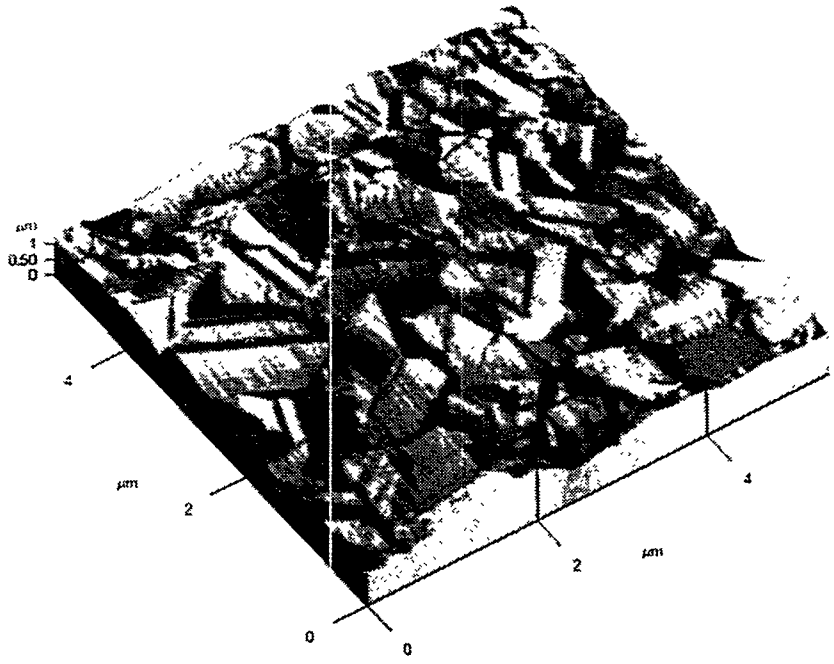

Figure 15. 3-D AFM image of good quality $CuIn_{1-x}Ga_xSe_2$ samples showing large, compact, well-faceted grains with crystallographic shapes

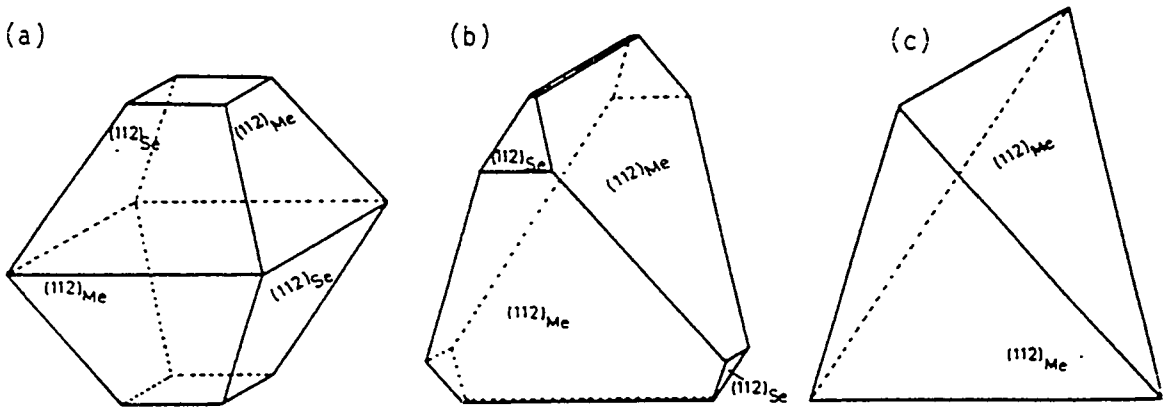

Figure 16. The most stable growth form of chalcogenides corresponding to the polyhedron

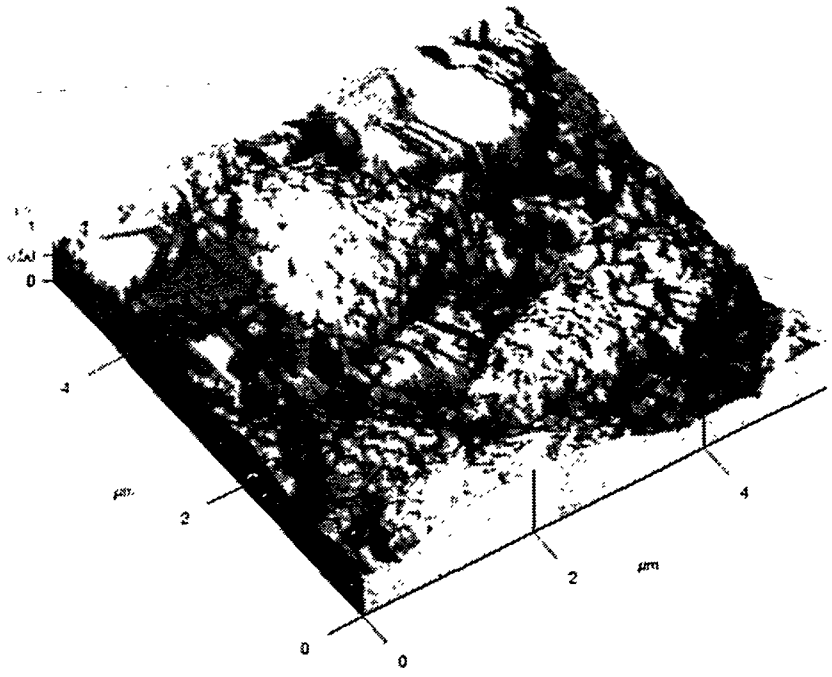

Figure 17. 3-D AFM image of a sample prepared at excessively high selenization temperature and with low selenium vapor incidence rate

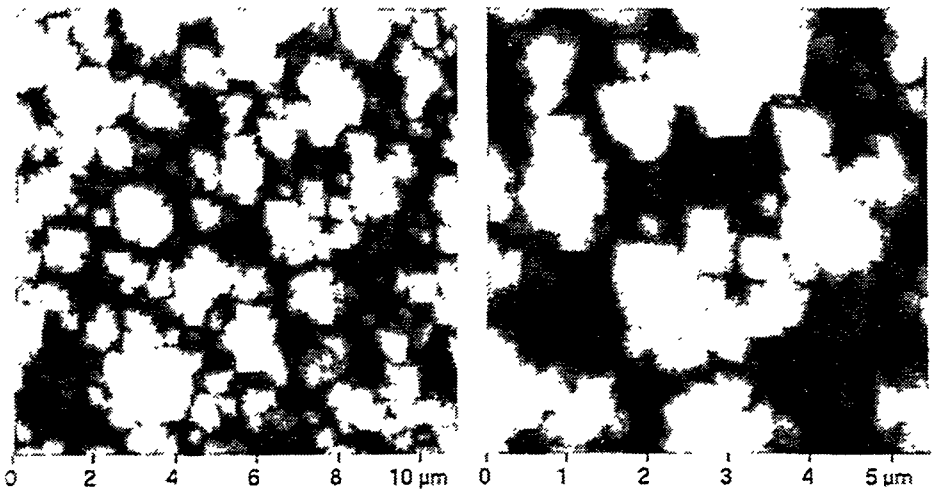

Figure 18. 2-D AFM image showing fine grain morphology of a sample consisting of only the second set of metallic precursors Cu-In-Ga deposited on glass/Mo substrate after undergoing a selenization at 500°C

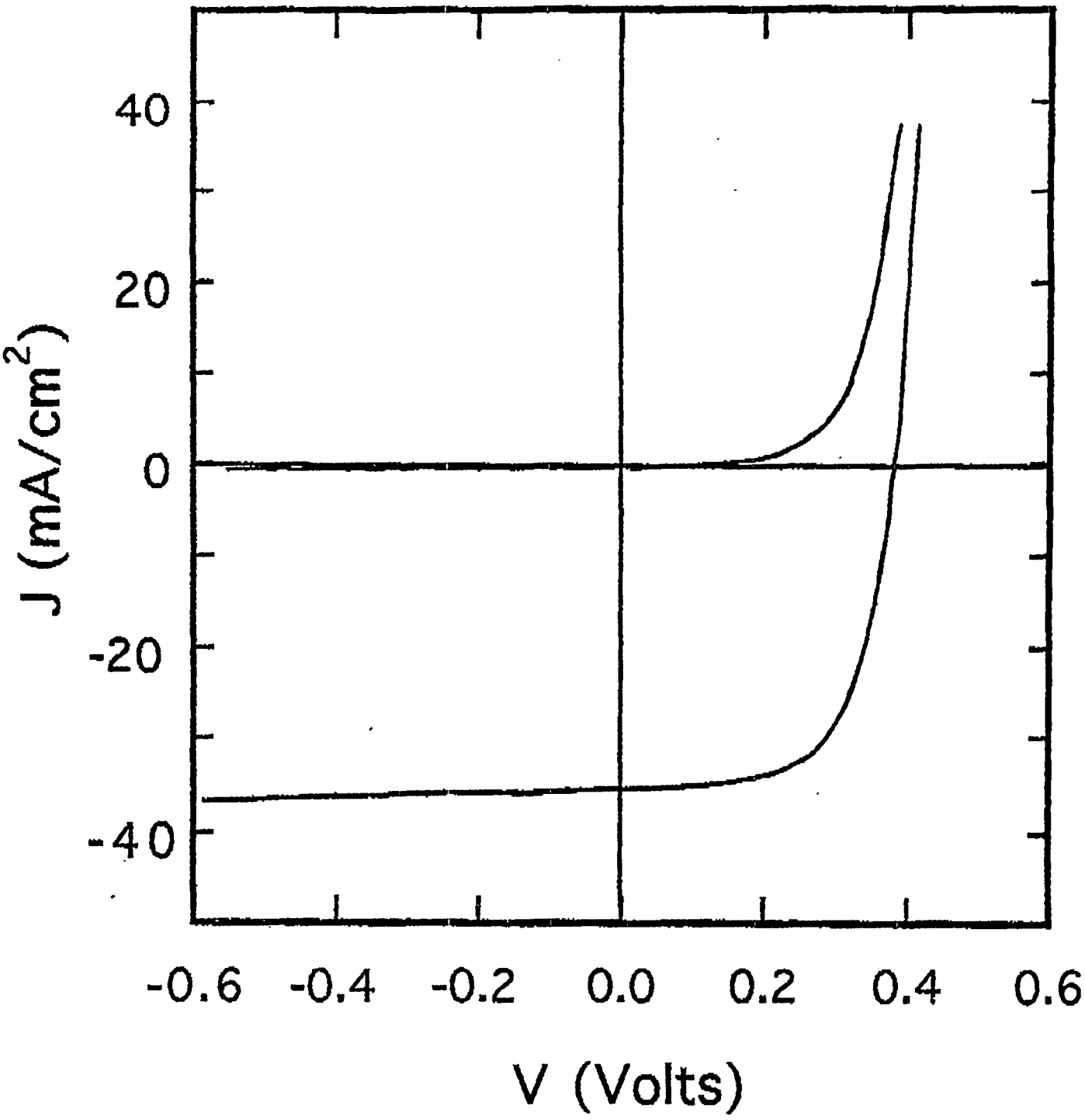

Fig. 19. IxV characteristic of $CuIn_{1-x}Ga_xSe_2$ thin-film solar cell

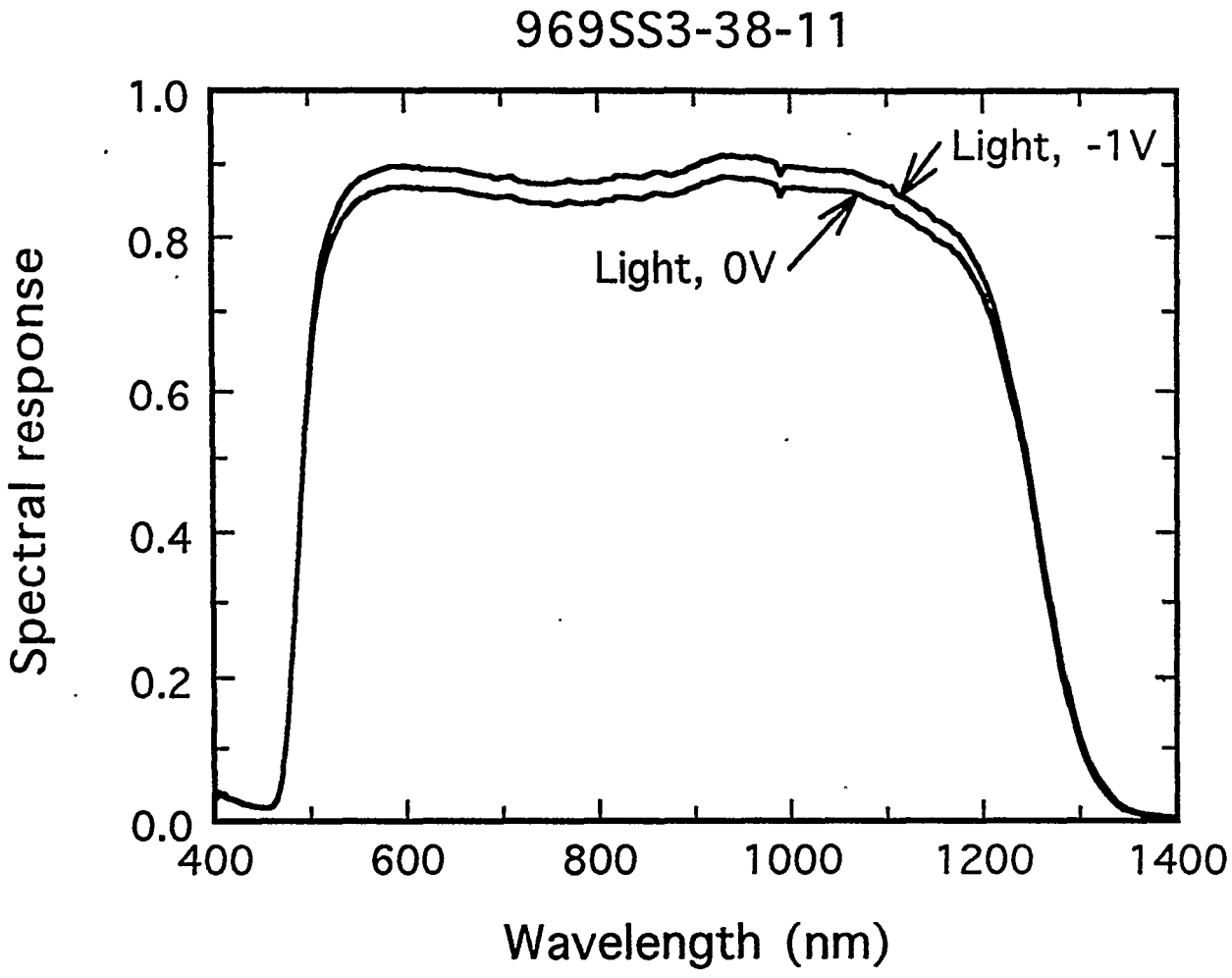

Fig. 20. Spectral response of $CuIn_{1-x}Ga_xSe_2$ thin-film solar cell

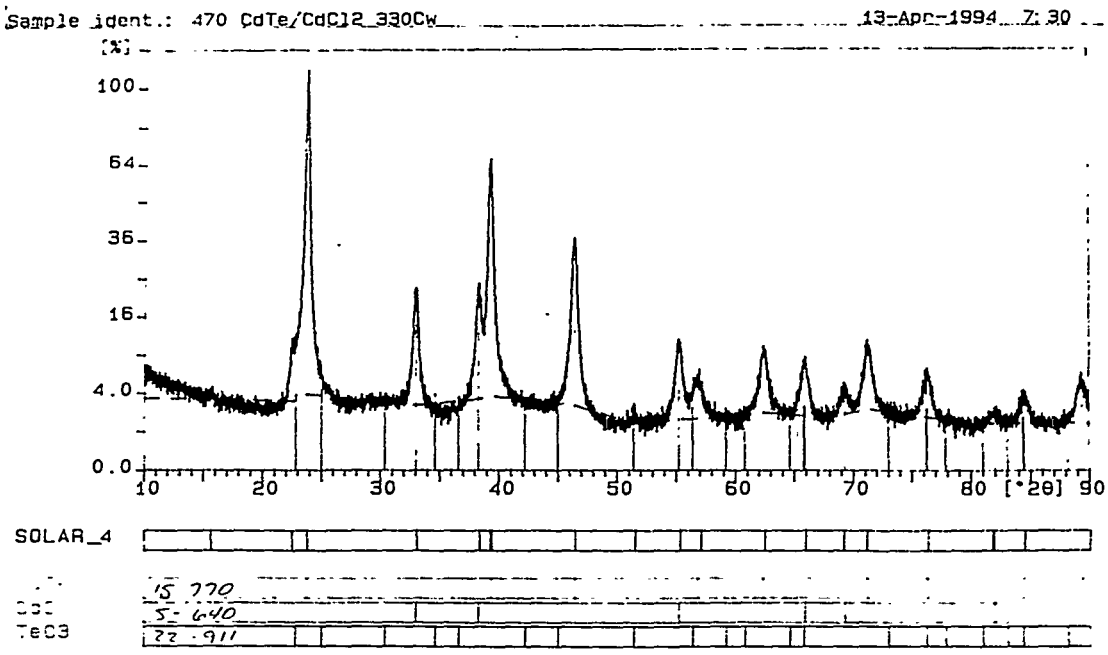

Fig. 21. XRD pattern of samples CdTe sample heat-treated at <280° C for 30 minutes

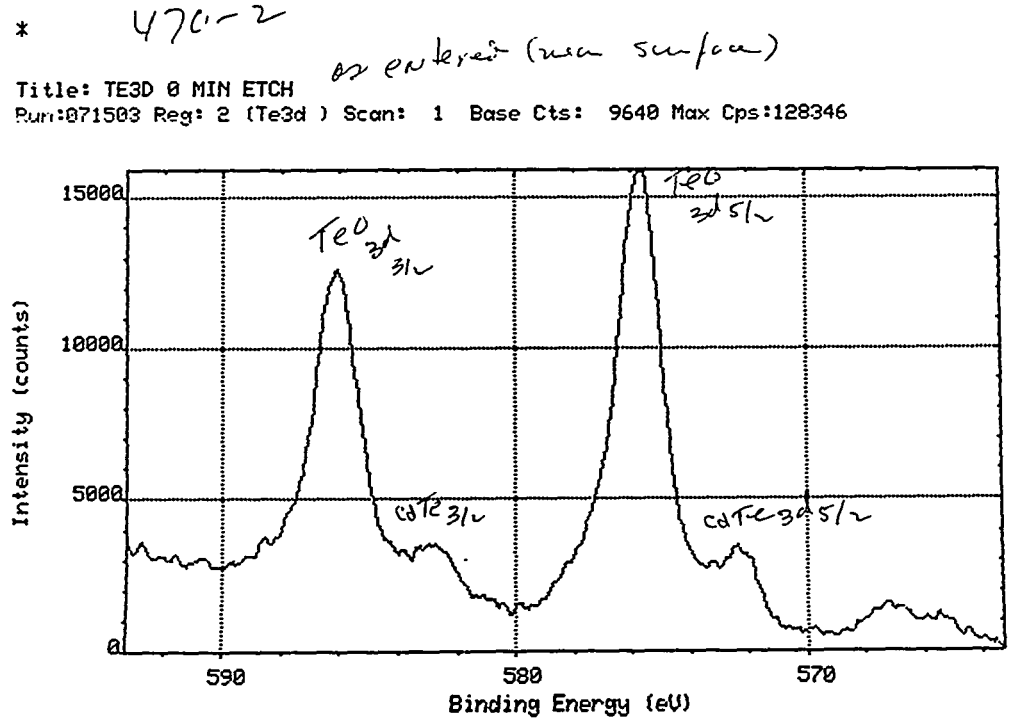

Fig. 22. XPS peaks from Te $3d_{3/2}$ and $3d_{5/2}$ incorporated as CdTe, and incorporated in TeO_x

* #470-1

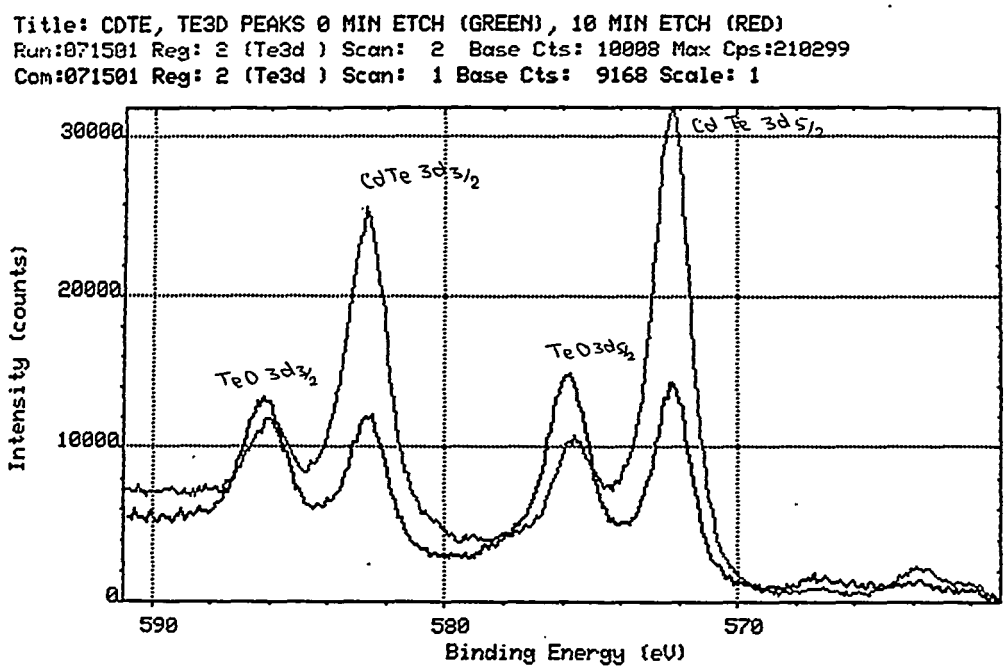

Fig. 23. XPS spectra of heat-treated CdTe sample, green curve corresponding to the surface (0 min etch) and red curve corresponding to sample etched for 10 min.

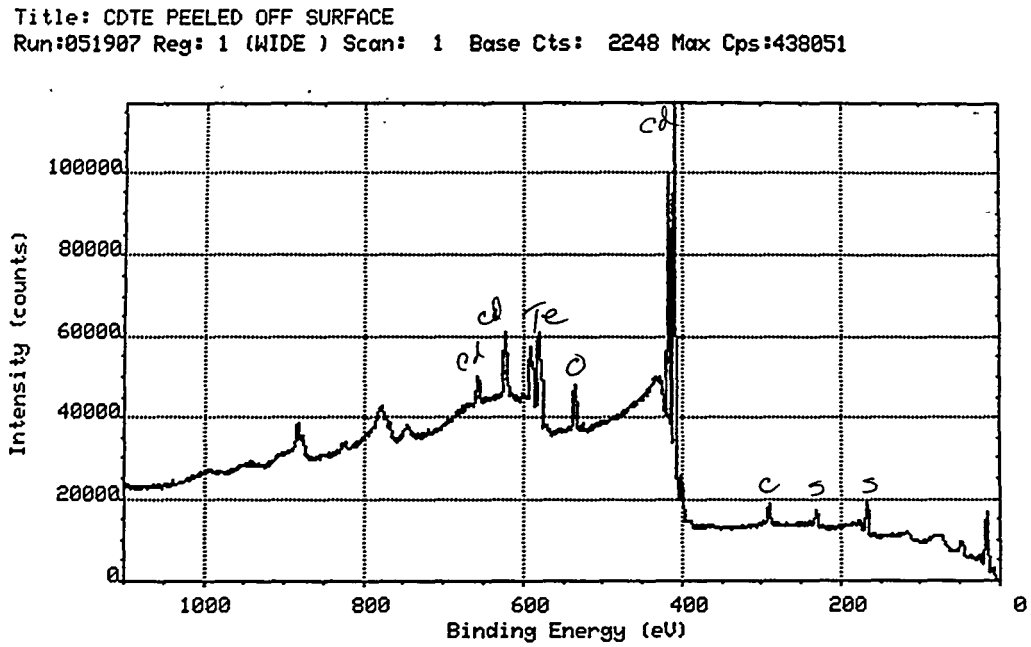

Fig. 24. XPS spectrum of the substrate below the peeled off CdTe film.

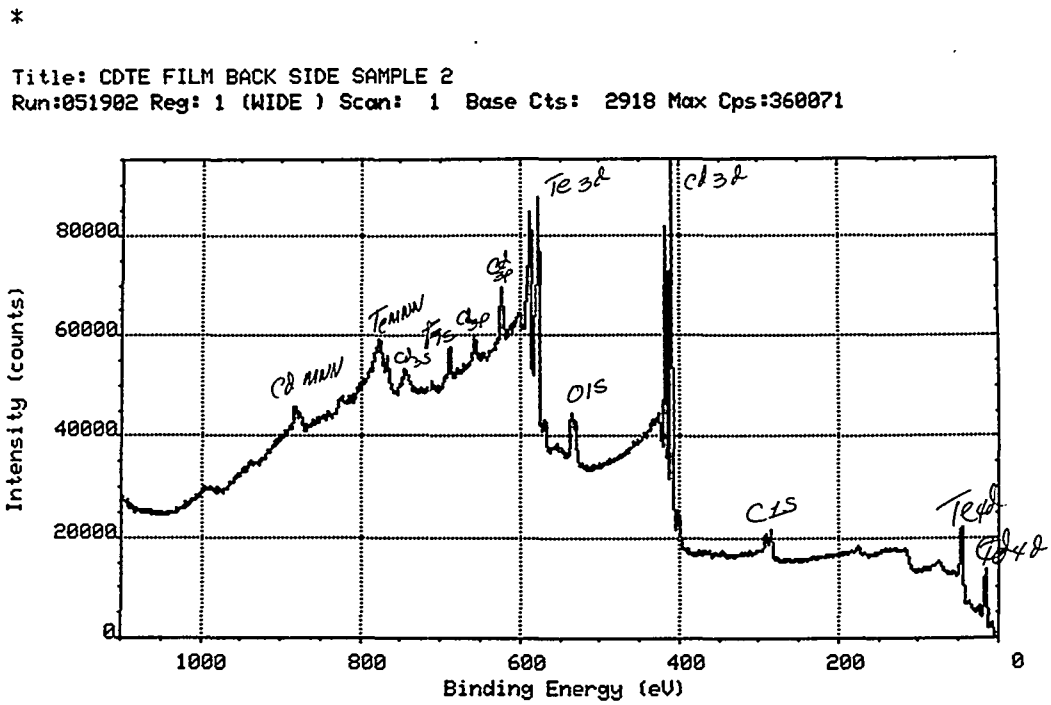

Fig. 25. XPS spectrum of the back side of the peeled off CdTe thin film

REPORT DOCUMENTATION PAGE

Form Approved
OMB NO. 0704-0188

1. AGENCY USE ONLY (Leave blank)	2. REPORT DATE	3. REPORT TYPE AND DATES COVERED
	November 1994	Annual Subcontract Report, 15 April 1993 - 14 April 1994

4. TITLE AND SUBTITLE

Polycrystalline $CuInSe_2$ and CdTe PV Solar Cells

5. FUNDING NUMBERS

C: XG-2-11036-5

TA: PV431101

6. AUTHOR(S)

N. G. Dhere

7. PERFORMING ORGANIZATION NAME(S) AND ADDRESS(ES)

Florida Solar Energy Center
300 State Road 401
Cape Canaveral, FL 32920

8. PERFORMING ORGANIZATION REPORT NUMBER

9. SPONSORING/MONITORING AGENCY NAME(S) AND ADDRESS(ES)

National Renewable Energy Laboratory
1617 Cole Blvd.
Golden, CO 80401-3393

10. SPONSORING/MONITORING AGENCY REPORT NUMBER

TP-451-7189

DE95000244

11. SUPPLEMENTARY NOTES

NREL Technical Monitor: B. von Roedern

12a. DISTRIBUTION/AVAILABILITY STATEMENT

12b. DISTRIBUTION CODE

UC-1263

13. ABSTRACT *(Maximum 200 words)*

This report describes work on Phase 1 of a 3-year research program. $CuIn_{1-x}Ga_xSe_2$ and CdTe polycrystalline thin-film solar cells are emerging as the leading candidates for meeting the DOE long-range cost goals. The Florida Solar Energy Center has established a well-equipped laboratory with hazardous material handling capabilities for research and development on thin-film solar cells. The principal objective of the research project is to develop novel and low-cost processes for the fabrication of stable and efficient $CuIn_{1-x}Ga_xSe_2$ and CdTe polycrystalline thin-film solar cells using reliable techniques amenable to scaling up for economic, large-scale manufacture. The aims are to develop a process for the non-toxic selenization so as to avoid the use of extremely toxic H_2Se in the fabrication of $CuIn_{1-x}Ga_xSe_2$ thin-film solar cells; to optimize selenization parameters; to develop a process for the fabrication of CdTe solar cells using Cd and Te layers sputtered from elemental targets; to develop an integrated process for promoting the interdiffusion between Cd/Te layers, CdTe phase formation, grain growth, type conversion, and junction formation; to improve adhesion; to minimize residual stresses; to improve the metallic back contact; to improve the uniformity, stoichiometry, and morphology of $CuIn_{1-x}Ga_xSe_2$ and CdTe thin films; and to improve the efficiency of $CuIn_{1-x}Ga_xSe_2$ and CdTe solar cells.

14. SUBJECT TERMS

copper indium diselenide ; cadmium telluride ; polycrystalline ; photovoltaics ; solar cells

15. NUMBER OF PAGES
43

16. PRICE CODE

17. SECURITY CLASSIFICATION OF REPORT	18. SECURITY CLASSIFICATION OF THIS PAGE	19. SECURITY CLASSIFICATION OF ABSTRACT	20. LIMITATION OF ABSTRACT
Unclassified	Unclassified	Unclassified	UL